cmgh
CELLULAR AND MOLECULAR GASTROENTEROLOGY AND HEPATOLOGY

ORIGINAL RESEARCH

Decrease in MiR-148a Expression During Initiation of Chief Cell Transdifferentiation

Takahiro Shimizu,[2,3,4,5,a] Yoojin Sohn,[3,4,a] Eunyoung Choi,[1,2,3,4] Christine P. Petersen,[2,3,4] Nripesh Prasad,[6] and James R. Goldenring[1,2,3,4]

[1]Nashville VA Medical Center, Nashville, Tennessee; [2]Department of Surgery and [3]Department of Cell and Developmental Biology and [4]Epithelial Biology Center, Vanderbilt-Ingram Cancer Center, Vanderbilt University School of Medicine, Nashville, Tennessee; [5]Department of Gastroenterology and Hepatology, Graduate School of Medicine, Kyoto University, Kyoto, Japan; and [6]HudsonAlpha Institute for Biotechnology, Huntsville, Alabama

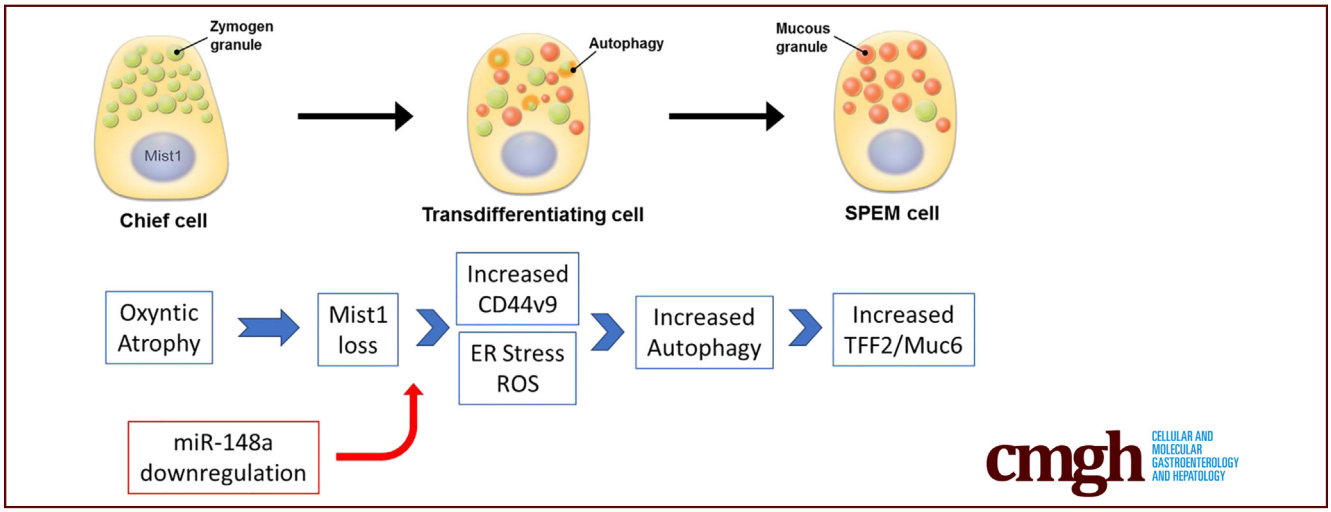

SUMMARY

Following parietal cell loss, chief cells transdifferentiate into mucous cell metaplasia, designated spasmolytic polypeptide-expressing metaplasia (SPEM). Induction of SPEM was associated with loss of miR-148a. Loss of miR-148a is an early step in chief cell transdifferentiation.

Gastric chief cells differentiate from mucous neck cells and develop their mature state at the base of oxyntic glands with expression of secretory zymogen granules. After parietal cell loss, chief cells transdifferentiate into mucous cell metaplasia, designated spasmolytic polypeptide-expressing metaplasia (SPEM), which is considered a candidate precursor of gastric cancer. We examined the range of microRNA (miRNA) expression in chief cells and identified miRNAs involved in chief cell transdifferentiation into SPEM. Among them, miR-148a was strongly and specifically expressed in chief cells and significantly decreased during the process of chief cell transdifferentiation. Interestingly, suppression of miR-148a in a conditionally immortalized chief cell line induced up-regulation of CD44 variant 9 (CD44v9), one of the transcripts expressed at an early stage of SPEM development, and DNA methyltransferase 1 (Dnmt1), an established target of miR-148a. Immunostaining analyses showed that Dnmt1 was up-regulated in SPEM cells as well as in chief cells before the emergence of SPEM in mouse models of acute oxyntic atrophy using either DMP-777 or L635. In the cascade of events that leads to transdifferentiation, miR-148a was down-regulated after acute oxyntic atrophy either in xCT knockout mice or after sulfasalazine inhibition of xCT. These findings suggest that the alteration of miR-148a expression is an early event in the process of chief cell transdifferentiation into SPEM. *(Cell Mol Gastroenterol Hepatol 2020;9:61–78; https://doi.org/10.1016/j.jcmgh.2019.08.008)*

Keywords: SPEM; miRNA; CD44 Variant 9; miR-148a; Transdifferentiation; Metaplasia; Gastric; DNMT1; Plasticity.

See editorial on page 189.

In the stomach mucosa, gastric chief cells are located at the base of oxyntic glands and express secretory zymogens. Chief cells differentiate from mucous neck cells in the lower half of corpus glands without cell division and remain in a fully differentiated state under normal conditions with a lifetime of more than 60 days.[1] Previous studies demonstrated that some transcription factors, including XBP1 and MIST1, are

required for the differentiation from mucous neck cells into chief cells and the maintenance of chief cells.[2–4] On the other hand, parietal cell loss and inflammation induce chief cells to transdifferentiate into mucous cell metaplasia, designated spasmolytic polypeptide-expressing metaplasia (SPEM), with the loss of zymogen granules and the formation of Muc6-containing mucous granules.[2,5] SPEM is considered a likely precursor lineage for intestinal metaplasia (IM) development,[3,6] and these metaplasias are possible precursor lesions of gastric cancer. However, the regulatory mechanisms for the chief cell transdifferentiation process have not been fully elucidated.

MicroRNAs (miRNAs) are critical post-transcriptional regulators of gene expression.[7,8] MiRNAs are involved in the developmental process of various organs as well as cancer progression.[9,10] Dysregulation of miRNAs has been reported in human gastric cancer[11] and *Helicobacter pylori*–induced gastritis,[12,13] contributing to gastric epithelial cell proliferation. We previously reported an analysis of miRNAs in laser capture microdissected human chief cells, SPEM cells, and IM cells, suggesting that miR-30a down-regulation and miR-194 up-regulation were related to metaplasia progression through regulation of the transcription factors HNF4γ and NR2F2.[14] However, it remains unclear whether miRNAs are involved in the initiation of SPEM development.

Chief cell transdifferentiation and the transition to SPEM cells occur through series of ordered events. Our group and others have identified a number of events that chief cells undergo to transdifferentiate from zymogen secreting cells into mucous secreting metaplastic cells. Acute oxyntic atrophy induces an early loss of the chief cell maturation-specifying transcription factor, Mist1,[15–17] and up-regulation of the specific splice variant of CD44, CD44 variant 9 (CD44v9).[17–19] CD44v9 is an activator and a stabilizer of xCT, a cystine transporter, which promotes adaptation to reactive oxygen species and cellular stress.[18–20] The increased cellular stress is associated with an increase in autophagy, which is necessary for breaking down the zymogen granules.[21] Importantly, the process of transdifferentiation can be arrested at different stages,[17,19,21] suggesting that chief cell transdifferentiation occurs through a set of stepwise events that are coordinated and maintained in a defined order.

Here we investigated the influence of miRNAs on the initiation of chief cell transdifferentiation into SPEM cells. We performed miRNA profiling specifically on mouse chief cells and compared miRNA expression with that in conditionally immortalized mouse chief cell and SPEM cell lines. Interestingly, several miRNAs were highly expressed in normal chief cells but down-regulated in SPEM cells. Among them, miR-148a was the most highly expressed miRNA by more than 10-fold in chief cells. Loss of miR-148a was associated with the early initiation of chief cell transdifferentiation. In addition, the loss of miR-148a led to up-regulation of an early SPEM marker, CD44 variant 9, and one of its target genes, DNA methyltransferase 1 (Dnmt1). The loss of miR-148a was found early during the chief cell transdifferentiation process, preceding up-regulation of CD44v9. These findings suggest that miR-148a is an early regulator in reprogramming chief cells during transdifferentiation into SPEM.

Results

MicroRNA Profile of In Vivo Mouse Chief Cells and Immortalized Chief Cell and Spasmolytic Polypeptide-Expressing Metaplasia Cell Lines

In a previous study, our group reported the miRNA profile of human SPEM and IM in comparison with chief cells from normal stomach.[14] In those studies, we identified miRNAs related with human IM progression; however, no miRNAs related to SPEM development were confirmed. We therefore sought to investigate miRNAs during the initiation of SPEM development by using mouse models. First, to profile miRNAs from mouse chief cells, we crossed Mist1$^{CreERT2/+}$mice with R26R^{mTmG} reporter mice. After tamoxifen injection, immunostaining analyses of these mouse stomachs showed that most of green fluorescent protein (GFP)-positive cells were chief cells at the base of glands, with only occasional labeled cells in the isthmus regions (Figure 1*A*).[1] We sorted GFP-positive cells from 2 mice and performed miRNA sequencing (Figure 1*B*). Forty-three miRNAs were highly expressed in mouse chief cells (read values >500 in both mice) (Table 1). Among them, miR-148a-3p was the most highly expressed miRNA (read values >150,000) in chief cells, more than 10-fold higher than other highly expressed miRNAs such as miR-375-3p, let-7 family (let-7b-5p, let-7c-5p, let-7f-5p and let-7a-5p), and miR-200b-3p (read values >8000). Interestingly, these miRNAs have already been reported as down-regulated in human gastric cancer tissues and related to gastric cancer progression.[22–25]

To investigate miRNAs related to metaplasia development, we examined miRNA expression profiles for conditionally immortalized mouse chief cell (ImChief) and SPEM cell (ImSPEM) lines, previously established from Immortomice.[26] ImChief cells express chief cell markers such as pepsinogen C (*Pgc*) and *Mist1* and produce characteristic zymogen granules, although they do not express gastric intrinsic factor (GIF). In contrast, ImSPEM cells express SPEM-specific markers such as *Tff2* and *He4* and some intestinalized markers such as *Cftr* and *PigR*. We extracted total RNAs from ImChief cells and ImSPEM cells and performed miRNA sequencing. We detected 87 miRNAs down-regulated ($P < .01$, with read values for ImChief cells >500 and fold-change >5) and 7 miRNAs up-regulated ($P < .01$, with read values for ImSPEM cells >500 and fold-change >5) in ImSPEM cells compared with ImChief cells (Tables 2 and 3). From these 2 different sequencing studies, we identified 15 miRNAs that were both highly expressed in

[a]Authors share co-first authorship.

Abbreviations used in this paper: DAPI, 4′,6-diamidino-2-phenylindol; DMEM, Dulbecco minimum essential medium; DNMT, DNA methyltransferase; GFP, green fluorescent protein; GIF, gastric intrinsic factor; GSII, *Griffonia simplicifolia* lectin II; IM, intestinal metaplasia; miRNA, microRNA; PCR, polymerase chain reaction; SPEM, spasmolytic polypeptide-expressing metaplasia.

Most current article

2352-345X
https://doi.org/10.1016/j.jcmgh.2019.08.008

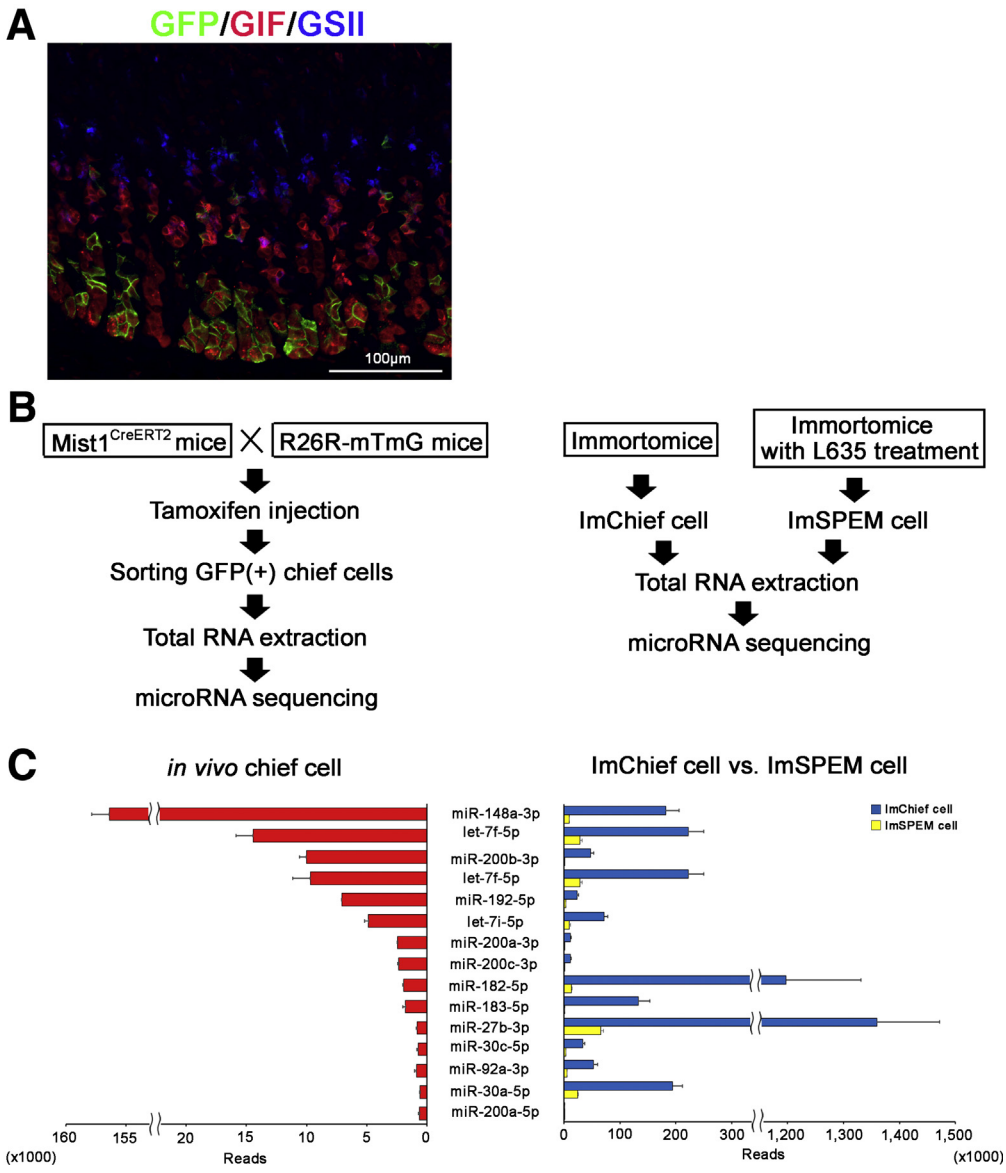

Figure 1. miRNAs related to SPEM development. (*A*) Immunofluorescence staining in Mist1$^{CreERT2/+}$;R26R$^{mTmG/+}$ mice. Membrane-associated GFP was expressed in GIF-positive chief cells and occasionally in the isthmus regions at 10 days after tamoxifen injection. (*B*) Schemes of miRNA sequencing experiments. (*left*) miRNAs from sorted chief cells of Mist1-mTmG mice. (*right*) miRNAs from ImChief cells and ImSPEM cells. (*C*) Fifteen miRNAs that were both highly expressed in sorted chief cells (*red*) and down-regulated in ImSPEM cells (*yellow*) compared with ImChief cells (*blue*). The read values for these miRNAs were more than 500, and fold changes of expression between ImSPEM cells and ImChief cells were more than 5. miRNA sequencing analyses detected 2 different let-7f-5p as up-regulated miRNAs in chief cells. Top one was at chromosome X, and another was at chromosome 13 (Table 1).

sorted chief cells and down-regulated in ImSPEM cells compared with ImChief cells (Figure 1*C*) as candidate miRNAs related to SPEM development. This group of miRNAs included miR-148a-3p, miR-200 family members (miR-200a-3p, miR-200a-5p, miR-200b-3p, and miR-200c-3p), miR-30 family members (miR-30a-5p and miR-30c-5p), and let-7 family members (let-7f-5p and let-7i-5p).

MiR-148a Expression in Mouse Stomach Assessed by In Situ Hybridization

Because it was by far the most highly expressed miRNA species in chief cells, we focused our subsequent studies on miR-148a. To examine the distribution of miR-148a expression, we performed in situ hybridization analyses for miR-148a (Figure 2). In normal stomach, miR-148a was strongly expressed in the bases of corpus glands, deep to *Griffonia simplicifolia* lectin II (GSII)-positive mucous neck cells, and surface cells and mucous neck cells showed no or very low expression of miR-148a (Figure 2*A*). MiR-148a expression was localized in the cytoplasm, especially in the basal side of cells. In contrast to the corpus, the antrum and the duodenum showed little or no expression of miR-148a. Importantly, dual immunostaining with in situ hybridization demonstrated that miR-148a–positive cells expressed the chief cell markers Mist1 and GIF (Figure 2*B*). Examination of Mist1$^{CreERT2/+}$;R26R$^{tdTomato/+}$ mice also showed that Mist1-positive chief cells have strong miR-148a expression (Figure 2*C*). These data suggest that miR-148a is strongly and specifically expressed in chief cells in the gastric corpus.

Next, to evaluate the alteration of expression of miR-148a during the development of SPEM, we examined in situ hybridization analyses in 2 mouse models of acute oxyntic atrophy (administration of either DMP-777 or L635). Compared with normal chief cells, miR-148a was down-regulated in

Table 1. MicroRNAs Highly Expressed in Mouse Chief Cells

Accession	Chromosome	Strand	Start	End	Gene ID	Sample 1	Sample 2	Entrez ID
mmu-miR-148a-3p	chr6	–	51219828	51219849	MI0000550_1	157846.9654	154942.4573	387166
mmu-miR-375-3p	chr1	–	74947235	74947256	MI0000792_1	35248.20084	21476.74894	723900
mmu-let-7b-5p	chr15	+	85537755	85537776	MI0000558_1	25949.91154	27815.42445	387245
mmu-let-7c-5p	chr16	+	77599917	77599938	MI0000559_1	15987.66912	22193.04491	387246
mmu-let-7c-5p	chr15	+	85537046	85537067	MI0000560_1	14821.59409	20835.45521	723966
mmu-let-7f-5p	chrX	+	1.48E+08	1.48E+08	MI0000563_1	13039.97967	15870.56644	387253
mmu-miR-7a-5p	chr13	–	58494202	58494224	MI0000728_2	11223.58539	6231.293692	723902
mmu-miR-200b-3p	chr4	–	1.55E+08	1.55E+08	MI0000243_1	9422.302927	10591.6593	387243
mmu-let-7a-5p	chr13	–	48633608	48633629	MI0000556_2	8746.256843	12009.56271	387244
mmu-miR-7a-5p	chr7	+	86033181	86033203	MI0000729_1	8740.205588	4823.681713	723884
mmu-let-7a-5p	chr9	+	41344815	41344836	MI0000557_1	8363.615366	11563.89665	723965
mmu-let-7f-5p	chr13	–	48633258	48633279	MI0000562_2	8230.526464	11138.08047	387252
mmu-miR-192-5p	chr19	+	6264857	6264877	MI0000551_1	7084.120318	7057.18444	387187
mmu-miR-21-5p	chr11	–	86397622	86397643	MI0000569_2	5868.145795	7696.271615	387140
mmu-miR-26a-5p	chr10	+	1.26E+08	1.26E+08	MI0000706_1	5001.537708	3946.313897	723962
mmu-miR-26a-5p	chr9	+	1.19E+08	1.19E+08	MI0000573_1	5001.537708	3946.313897	387218
mmu-let-7i-5p	chr10	–	1.22E+08	1.22E+08	MI0000138_2	4517.566115	5195.810144	387251
mmu-miR-99a-5p	chr16	+	77599185	77599206	MI0000146_1	3504.250029	3589.631416	387229
mmu-miR-30d-5p	chr15	–	68172819	68172840	MI0000549_2	2757.120297	2825.520615	387228
mmu-miR-7b-5p	chr17	+	56382440	56382462	MI0000730_1	2657.301111	1373.046719	723883
mmu-miR-200a-3p	chr4	–	1.55E+08	1.55E+08	MI0000554_1	2465.225664	2397.499834	387242
mmu-miR-200c-3p	chr6	–	1.25E+08	1.25E+08	MI0000694_1	2239.877318	2418.092972	723944
mmu-miR-182-5p	chr6	–	30115962	30115986	MI0000224_2	2006.965359	1888.583689	387177
mmu-miR-1a-3p	chr18	–	10785483	10785504	MI0000652_1	1755.906123	63.24694981	723959
mmu-miR-125a-5p	chr17	+	17967781	17967804	MI0000151_1	1663.648576	1174.480463	387235
mmu-let-7g-5p	chr9	+	1.06E+08	1.06E+08	MI0000137_1	1585.004257	1562.052254	387249
mmu-miR-183-5p	chr6	–	30119711	30119732	MI0000225_2	1533.581369	2018.018941	387178
mmu-miR-151-3p	chr15	–	73085250	73085270	MI0000173_1	1308.233185	1660.600129	387169
mmu-miR-215-5p	chr1	+	1.87E+08	1.87E+08	MI0000974_1	1215.975967	3101.305644	387211
mmu-miR-127-3p	chr12	+	1.11E+08	1.11E+08	MI0000154_2	1188.753604	600.1103493	387146
mmu-miR-143-3p	chr18	–	61808853	61808873	MI0000257_1	1025.412731	771.4655906	387161
mmu-miR-378-3p	chr18	–	61557492	61557512	MI0000795_1	1020.875345	2281.30322	723889
mmu-miR-423-5p	chr11	–	76891624	76891646	MI0004637_2	1001.21424	1177.423	751519
mmu-miR-27b-3p	chr13	+	63402068	63402088	MI0000142_2	860.560016	781.7616481	387221
mmu-miR-30c-5p	chr1	+	23298553	23298575	MI0000548_1	852.9982668	620.7028672	723964
mmu-miR-30c-5p	chr4	–	1.2E+08	1.2E+08	MI0000547_2	848.4606843	617.0253704	387227
mmu-miR-92a-3p	chr14	+	1.15E+08	1.15E+08	MI0000719_2	739.5680038	1023.717545	751549
mmu-let-7e-5p	chr17	+	17967330	17967351	MI0000561_1	680.5837996	718.5145194	387248
mmu-let-7d-5p	chr13	–	48631447	48631468	MI0000405_2	603.4510756	628.792413	387247
mmu-miR-30a-5p	chr1	+	23279113	23279134	MI0000144_1	586.8142113	556.7203464	387225
mmu-miR-320-3p	chr14	+	70843364	70843385	MI0000704_2	580.7647177	527.3028558	723838
mmu-miR-25-3p	chr5	–	1.39E+08	1.39E+08	MI0000689_1	552.0292875	714.1023224	723926
mmu-miR-200a-5p	chr4	–	1.55E+08	1.55E+08	MI0000554_2	547.491972	686.8912993	387242

GSII-positive SPEM cells in mice after 10 days of DMP-777 treatment or 3 days of L635 treatment (Figure 3*A*). Importantly, miR-148a was down-regulated in chief cells without GSII expression after 3 days of DMP-777 treatment or 1 day of L635 treatment. Fluorescence intensity was measured for quantitation, and miR-148a expression was decreased significantly in mice with 10 days of DMP-777 treatment or 3 days of L635 treatment (Figure 3*B*). We also examined miR-148a expression by in situ hybridization in mice infected with *Helicobacter felis*, and mice infected with *H felis* for 6 months and 12 months showed decreased levels of miR-148a expression (Figure 3*C* and *D*). These findings suggest that the down-regulation of miR-148a could be involved in the chief cell transdifferentiation into SPEM cells.

Table 2. MicroRNAs Down-regulated in ImSPEM Cells Compared With ImChief Cells

Feature	ImSPEM cells_1	ImSPEM cells_2	ImSPEM cells_3	ImChief cells_1	ImChief cells_2	ImChief cells_3	ImSPEM cells/ImChief cells
mmu-miR-141-5p	0	0	0	1005	1576	1593	0
mmu-miR-141-3p	60.5	75.5	84	147862	151753	220628.5	0.000423
mmu-miR-200c-3p	7	6	3	8326.5	13315	12489.5	0.000469
mmu-miR-205-5p	145	148	197	233099	355470	318724	0.00054
mmu-miR-205-3p	5	5	3	4571	5175	5850	0.000834
mmu-miR-203-3p	8	11	11	4932	6346	6065	0.00173
mmu-miR-672-5p	1	2	4	1015	1430	1390	0.001825
mmu-miR-676-3p	2	2	2	682	735	856	0.00264
mmu-miR-429-3p	60	69	73	18745.5	22299.5	23313.5	0.003139
mmu-miR-146a-5p	136.5	163.5	172.5	28169.5	67458.5	42172	0.003429
mmu-miR-200a-3p	42.5	40.5	46	9297	12749	13597.5	0.003619
mmu-miR-200b-3p	239	269	316	37915	48814.5	56526	0.005752
mmu-miR-135b-5p	6	16	17	1674.67	2275.83	2806.67	0.005772
mmu-miR-200a-5p	12	5	3	624	1067	745	0.00821
mmu-miR-183-5p	1153	1362	1308	109600	114757	173820	0.009601
mmu-miR-183-3p	11	14	13	1045	1147	1645	0.009904
mmu-miR-182-5p	15006	12308	14206	1002426	1136518	1453717	0.011557
mmu-miR-96-5p	98	112	92	6537	7080	10821	0.012358
mmu-miR-193b-3p	67	108	94	3006	2259	5077.5	0.026009
mmu-miR-31-3p	24	82	48	1569	1446	2632	0.027271
mmu-miR-31-5p	6738	5724	7552	182407	217916	244071	0.031059
mmu-miR-582-3p	32	21	48	844	905	1241	0.033779
mmu-miR-421-3p	167	192	226	4175	4981	5907	0.038837
mmu-miR-147-3p	26	18	28	427	604	599	0.044172
mmu-miR-222-3p	2279	1489	2261	32959	50742	47026	0.046119
mmu-miR-210-5p	39	46	64	684	1217	1212	0.047864
mmu-miR-27b-3p	58480	65172.5	74847.5	1248916	1245684	1584584	0.048662
mmu-miR-181b-5p	563	509.5	742.67	10536.83	12984.17	13485.67	0.04905
mmu-miR-181a-5p	7652	7487	8969	142888	140394	203123	0.049564
mmu-miR-148a-3p	8590.5	9828.5	9697.5	140196	181813	223713.5	0.051522
mmu-miR-148a-5p	67	66	78	1008	1140	1544	0.057151
mmu-miR-298-5p	770	630	794	10712	10690	15097	0.060111
mmu-miR-21a-3p	480	1124	901	7385	10894	16739	0.071535
mmu-miR-101b-3p	142.5	211	182	1863.5	2280	2870.5	0.076347
mmu-miR-27b-5p	82	85	100	965	1248	1267	0.076724
mmu-miR-126a-5p	212	406	383	3065	4248	5532	0.077929
mmu-miR-1843a-5p	85	103	117	1180	1189	1462	0.079614
mmu-miR-365-3p	64	129	103	1071	917	1658	0.081185
mmu-miR-221-3p	2572	2973	3118	27309	32974	39637	0.086699
mmu-miR-29b-3p	151.67	274	211	1543.33	2317	2887.33	0.094354
mmu-miR-30c-5p	2801	3116	3936	29133.67	30398.33	40878	0.098128
mmu-miR-92a-3p	5585	4445.33	5511.67	42970.67	47225.33	66885.67	0.098942
mmu-miR-194-5p	165	136	242	1465	2072	1948	0.098997
mmu-miR-425-5p	346	436	499	3521	4204	4789	0.102365
mmu-miR-19b-3p	301.5	369.5	309.5	2310.17	3555.5	3663.5	0.102895
mmu-miR-221-5p	607	297	339	3409	3600	5063	0.102966
mmu-miR-374b-5p	55	100	130	744	914	1025	0.106224
mmu-miR-126a-3p	53	49	76	387	561	665	0.110353
mmu-miR-17-5p	101	130	130	830	1150.83	1259.83	0.111397

Table 2. Continued

Feature	ImSPEM cells_1	ImSPEM cells_2	ImSPEM cells_3	ImChief cells_1	ImChief cells_2	ImChief cells_3	ImSPEM cells/ImChief cells
mmu-miR-328-3p	160	152.5	210.5	1513	1110.5	1946.5	0.114442
mmu-miR-130b-3p	119	112.5	176	629.5	1266.5	1656	0.114724
mmu-miR-19a-3p	57.5	63.5	55.5	363.83	552.5	615.5	0.115222
mmu-miR-484	1241	1134	1489	9205	9226	14465	0.117461
mmu-miR-20a-5p	84	113	84	570	774	887.33	0.125934
mmu-miR-23b-3p	1793.5	3092	2818.5	17506	18406.5	25082	0.126306
mmu-miR-30a-5p	22727.5	24771	26421.5	164380	193723.5	225365.3	0.126691
mmu-miR-30e-5p	10724.5	10780.5	11758.5	70581	89679	98109.33	0.128744
mmu-miR-192-5p	2938	2785	3313.5	20230	21444	27916.5	0.129852
mmu-let-7f-5p	22306.05	28289.77	35971.93	174340.2	270159	221880.1	0.129908
mmu-miR-210-3p	846	949	1217	6351	7870	8930	0.130102
mmu-miR-22-3p	107186	109978	146919	737758	925662	1022961	0.135529
mmu-miR-107-3p	182.5	186.33	225.67	1261.83	1418	1703.83	0.135617
mmu-let-7i-5p	7772	9401	12263.5	59123	79414.5	77297.5	0.136384
mmu-miR-191-5p	13618	16310	18084	97568	100312	151097	0.137579
mmu-miR-98-5p	514.27	1025.47	1211.27	4932.67	7444.4	7119.93	0.141099
mmu-miR-34b-5p	444.5	548	642	3035.5	4005.5	4381	0.143101
mmu-miR-93-5p	4297	4794	5926	31000	32748	40799	0.143639
mmu-let-7b-3p	63	87	108	539	443	811	0.143893
mmu-let-7j	980.5	966.5	1326	6196	8255.5	8213.5	0.144408
mmu-miR-99b-3p	104	119	123	625	822.5	854	0.150337
mmu-miR-30a-3p	357	445	506.5	2347.5	2619.5	3139.5	0.161414
mmu-miR-24-3p	3038	3982	3287	16617	22764	24253	0.161973
mmu-miR-27a-3p	4684	6406.5	7145.5	31267	36340	43419.5	0.164249
mmu-miR-34b-3p	347	405	567	2219	2505	3299	0.164402
mmu-miR-342-3p	179	159	162	899	732	1409	0.164474
mmu-miR-1839-5p	194	235	293	1243	1427	1642	0.16744
mmu-miR-130a-3p	2613	2714.5	3310	13909.5	17149.5	20256	0.168323
mmu-miR-140-3p	616	798	807	3466	4682	5039	0.168423
mmu-miR-29a-3p	5652.5	5820	6999	28115.5	38135.5	42291.83	0.170177
mmu-miR-450b-5p	310	290	330	1263	1804	2195	0.176739
mmu-miR-34c-5p	19682.5	20120	26912	100916.5	127993	144827	0.178507
mmu-miR-351-5p	2316	1802	1999	9210	9920	15121	0.178593
mmu-miR-34c-3p	126	327	317	1091	1488	1633	0.182811
mmu-miR-28a-3p	157	207	307	942	1264	1400	0.186079
mmu-miR-28a-5p	611	711	929	3248	4056	4324	0.193584
mmu-miR-186-5p	5336	5697	6401	23436	30215	36028	0.194404
mmu-let-7d-3p	387	589	647	2297	2030	3951	0.196062

MiR-148a Expression in Human Stomach Assessed by In Situ Hybridization

To assess whether the alteration in miR-148a expression was related to SPEM development in humans, we performed in situ hybridization analyses for miR-148a using human stomach tissue (Figure 4). The human stomach tissue section shown in Figure 4 conveniently contained normal corpus glands and SPEM glands side-by-side, allowing for clear comparison of expression between them. The miR-148a was exclusively expressed in chief cells located at the base of the normal corpus glands below the GSII-positive mucous neck cells. The SPEM glands, marked with GSII-positive staining to the base of the glands, had no or very low expression of miR-148a. This finding confirmed the down-regulation of miR-148a expression in SPEM in human stomach.

Involvement of MiR-148a in Initiation of Chief Cell Transdifferentiation

ImChief cells and ImSPEM cells grow continuously at the permissive temperature of 33°C because of their expression of temperature-dependent T antigen. However, at the non-

Table 3. MicroRNAs Up-regulated in ImSPEM Cells Compared With ImChief Cells

Feature	ImSPEM cells_1	ImSPEM cells_2	ImSPEM cells_3	ImChief cells_1	ImChief cells_2	ImChief cells_3	ImSPEM cells/ImChief cells
mmu-miR-10b-5p	255958.5	248754.5	263925	69.5	107.5	118.5	2601.144
mmu-miR-199a-5p	1767	1715	2536	6	8	18	188.0625
mmu-miR-199a-3p mmu-miR-199b-3p	2801	6977	7968	47	48	58	115.9869
mmu-miR-344d-3p	587	491	675	3	6	11	87.65
mmu-miR-10a-5p	60241.5	55707.5	59273	3125.5	3297.5	5008.5	15.328
mmu-miR-155-5p	887	1304	1593	164	199	235	6.327759
mmu-miR-181c-5p	561	590	657	213	267	328	2.237624

permissive temperature (39°C), the temperature-sensitive T antigen misfolds and thus no longer immortalizes the cells. Thus, ImChief cells and ImSPEM cells become more primary-like at the non-permissive temperature.[26] To investigate the role of miR-148a in chief cell plasticity, we examined these cell lines incubated at the non-permissive temperature for 72 hours. First, to confirm the expression levels of miR-148a in ImChief cells and ImSPEM cells, the expression of miR-148a was detected by microRNA assay, and miR-148a expression in ImSPEM cells was significantly lower than in ImChief cells (Figure 5*A*).

To investigate whether down-regulation of miR-148a is related to SPEM development, we examined the influence of inhibitors for miR-148a in ImChief cells. ImChief cells were transfected with miR-148a inhibitors and then incubated at 33°C overnight, followed by incubation at 39°C for 72 hours. The expression of miR-148a was significantly down-regulated in ImChief cells treated with the inhibitor (Figure 5*B*). Known chief cell and SPEM cell marker expression was examined by quantitative reverse transcription polymerase chain reaction (PCR), and ImChief cells treated with miR-148a inhibitor showed significant up-regulation of the variant 9 splice isoform of *Cd44* (*Cd44v9*), an early marker of SPEM,[18,19] although *Tff2* expression was not detected (Figure 5C). The expression of *Sox9* and *Clusterin* (*Clu*), other SPEM-associated markers, was increased, but not significantly (Figure 5*C*). The expression of chief cell specific genes, such as *Mist1* and *Pgc,* was not significantly changed. These data suggest that down-regulation of miR-148a could be involved in initiation of chief cell transdifferentiation.

DNA Methyltransferase 1 Up-regulation in Chief Cells During Chief Cell Transdifferentiation via Down-regulation of MiR-148a

We have previously examined genes related to the emergence of SPEM by investigating microarray assay for mRNA expression for RNA extracted from SPEM regions in gastrin-deficient mice treated with DMP-777 for 1 day or 3 days.[27] To investigate the direct linkage of changes in miRNA expression with the emergence of SPEM, we compared the candidate miR-148a target gene list with previous mRNA microarray data (Table 4). Interestingly, *Ccnf*, *Dgcr8*, *Dnmt1*, *Kat7*, and *Rcc2* were identified as possible targets of miR-148a during the transdifferentiation process of chief cells into SPEM cells; all were predicted by 3 different miRNA databases: microRNA.org, TargetScan, and miRDB.

To confirm the miR-148a regulation of these possible target genes, mRNA expression was examined in ImChief cells transfected with control inhibitor or miR-148a inhibitor. As expected from miRNA database prediction, most of the candidate target genes showed up-regulation of mRNA expression with miR-148a inhibition, including *Ccnf*, *Dgcr8*, *Dnmt1,* and *Rcc2* (Figure 5*D*). Among the putative target genes, we focused on Dnmt1, one of the DNA methyltransferases that is essential for the maintenance of DNA methylation. Several studies have validated that miR-148a directly targets Dnmt1 3′-untranslated region in various cells, including gastric cancer cells, contributing to tumor progression.[28–30] To confirm the expression of Dnmt1 in mouse stomach, we performed immunostaining analyses. In normal corpus, Dnmt1 was strongly expressed in isthmus cells and mucous neck cells (Figure 6*A*). Dnmt1-positive isthmus cells were positive for Ki67, but Dnmt1-positive mucous neck cells were negative for Ki67. In contrast, chief cells and parietal cells showed little or no detectable expression of Dnmt1. In mice with DMP-777 or L635 treatment, Dnmt1 was clearly up-regulated in SPEM cells as well as in chief cells before SPEM development (Figure 6*B* and *C*), and 40%–60% Dnmt1-positive cells were also proliferative (Figure 6*B* and *D*). These results suggest that the up-regulation of Dnmt1 in chief cells via miR-148a down-regulation could be involved in the initiation of chief cell transdifferentiation.

MiR-148a Down-regulation During the Chief Cell Transdifferentiation Process

Chief cell transdifferentiation occurs through coordinated stepwise events, and the process of transdifferentiation can be arrested at different steps. Our group recently showed that inhibition of the cystine transporter xCT by sulfasalazine treatment or xCT knockout arrests chief cell transdifferentiation process and prevents development of SPEM in mouse models of acute oxyntic atrophy.[19] It was also shown that xCT deficiency blocks chief cell transdifferentiation

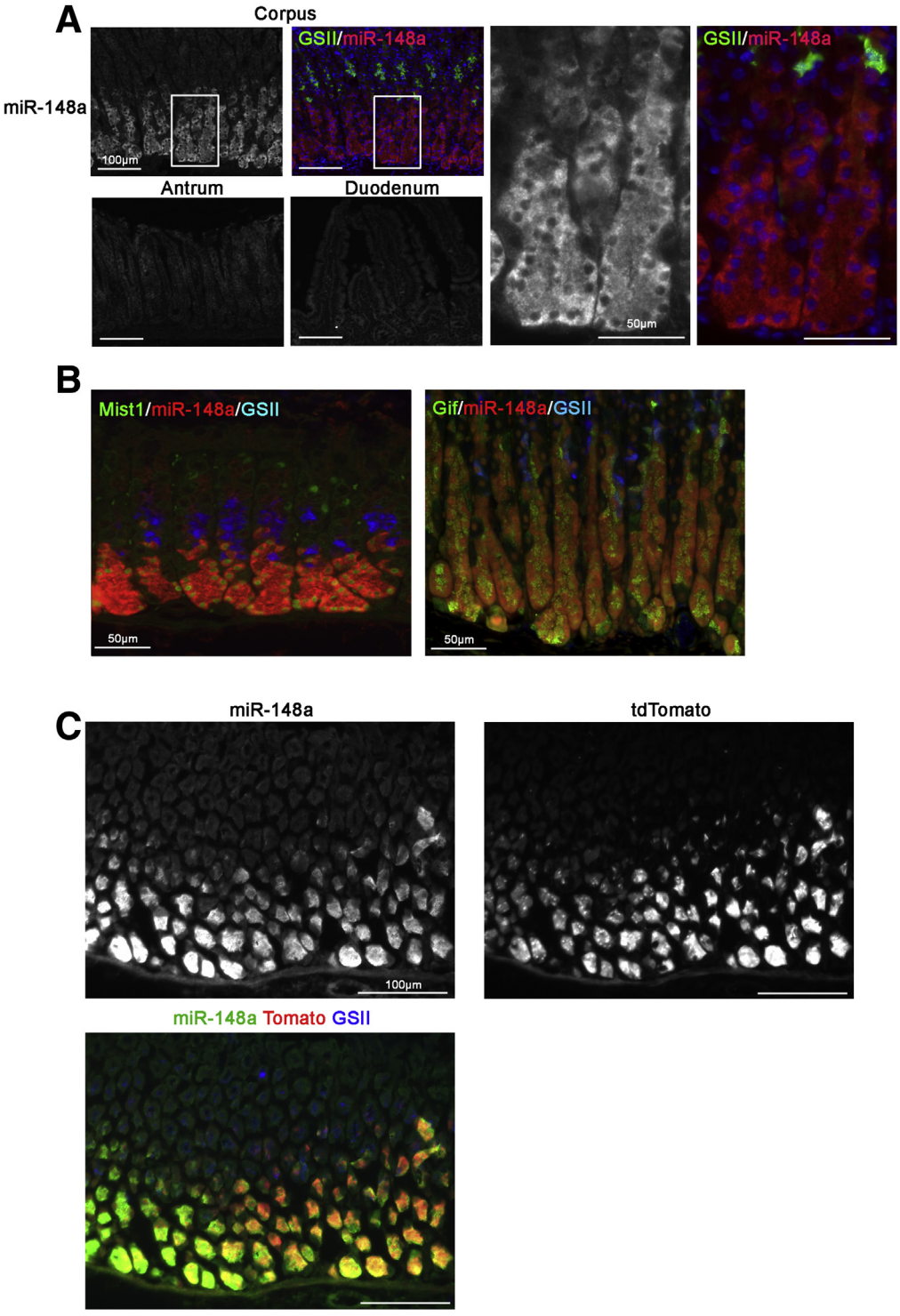

Figure 2. miR-148a expression in normal mouse stomach. (*A*) Fluorescence in situ hybridization for miR-148a (*red*) and immunofluorescence staining for GSII (*green*) and DAPI (*blue*). miR-148a was strongly expressed in the base of corpus glands deep to GSII-positive mucous neck cells. miR-148a expression was localized in the cytoplasm. No or little expression of miR-148a was seen in antrum and duodenum. (*B*) Fluorescence in situ hybridization for miR-148a (*red*) and immunofluorescence staining for GSII (*blue*) and Mist1 or GIF (*green*). miR-148a–positive cells expressed Mist1 and GIF. (*C*) Fluorescence in situ hybridization for miR-148a using $Mist1^{CreERT2/+}$; $R26R^{tdTomato/+}$ mice. miR-148a (*green*), tdTomato (*red*), and GSII (*blue*). miR-148a was expressed in tdTomato-positive chief cells.

process at a distinct step where the initiating step of Mist1 loss in chief cell reprogramming is not affected, but up-regulation of CD44v9 and autophagy that occur during chief cell transdifferentiation are blocked. To investigate where in this process miR-148a down-regulation occurs, we used these mouse models of xCT deficiency.[19] In mice treated with sulfasalazine only, miR-148a was expressed normally in chief cells, whereas co-treatment with sulfasalazine and 3 days of L635 resulted in loss of miR-148a (Figure 7*A* and *B*). In xCT knockout mice, untreated stomach exhibited similar expression of miR-148a as in wild-type mice, with expression in chief cells at the gland base, whereas 3 days of L635 treatment resulted in a significant down-regulation of miR-148a expression (Figure 7*C* and *D*). These results suggest that,

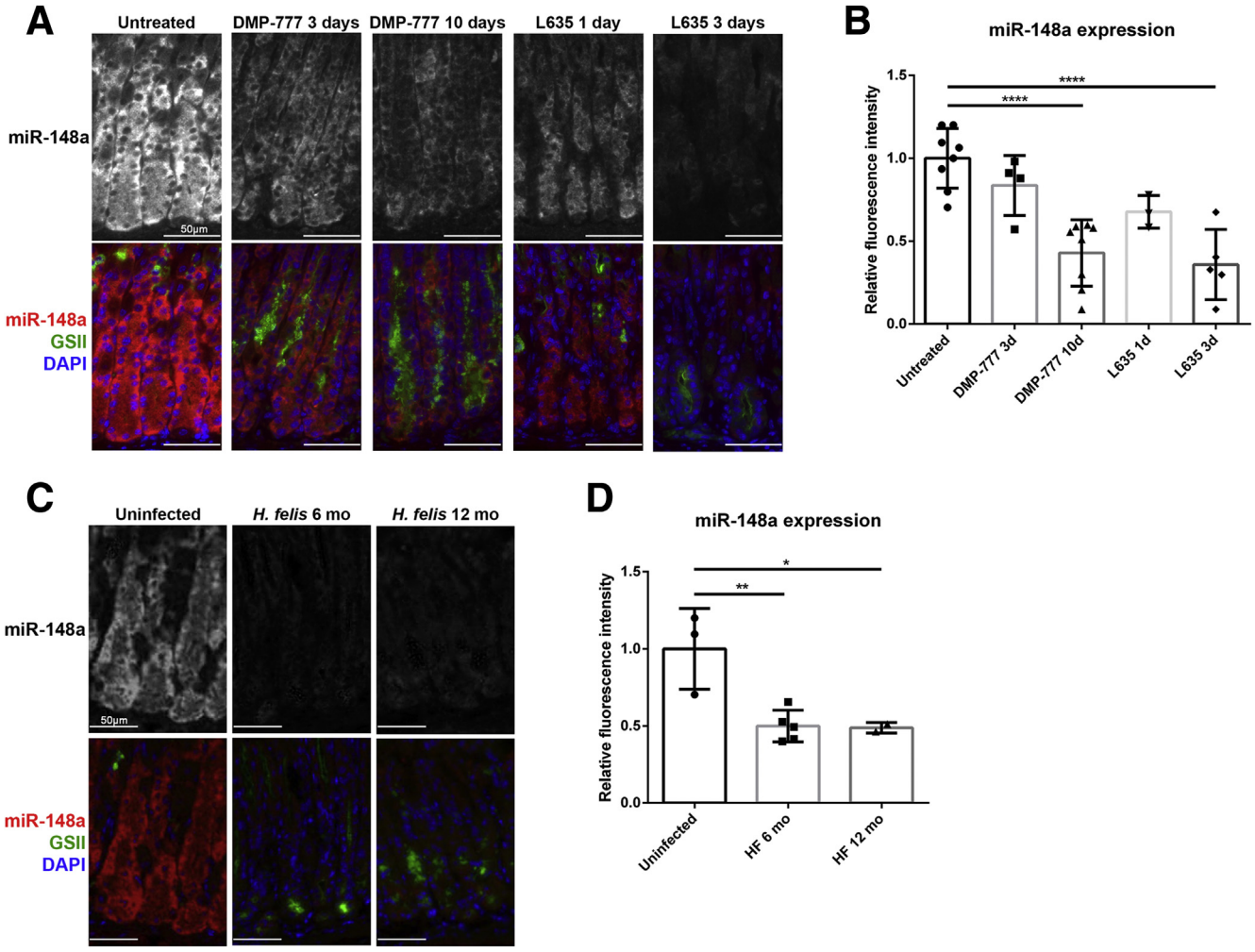

Figure 3. miR-148a expression during chief cell transdifferentiation into SPEM cells. (*A*) Fluorescence in situ hybridization for miR-148a (*red*) and immunofluorescence staining for GSII (*green*) and DAPI (*blue*). miR-148a was significantly down-regulated in GSII-positive SPEM cells developed in mice after 10 days of DMP-777 treatment or 3 days of L635 treatment as well as in chief cells without GSII expression after 3 days of DMP-777 treatment or 1 day of L635 treatment, compared with normal chief cells. (*B*) Quantitation of relative miR-148a staining intensity in chief cells and transdifferentiating chief cells at the base of the gland. One-way analysis of variance, $P < .0001$. Bonferroni multiple comparisons, $^{****}P < .0001$. (*C*) Fluorescence in situ hybridization for miR-148a (*red*) and immunofluorescence staining for GSII (*green*) and DAPI (*blue*). miR-148a was significantly decreased in GSII-positive SPEM cells developed in mice 6 months or 12 months after *H felis* infection. (*D*) Quantitation of relative miR-148a staining intensity in chief cells and *H felis* infection induced SPEM cells at the base of the gland. One-way analysis of variance, $P = .0081$. Bonferroni multiple comparisons, $^{*}P < .05$, $^{**}P < .01$.

like Mist1, the loss of miR-148a cannot be rescued with xCT deficiency, and miR-148a down-regulation most likely occurs early in the initiating step of chief cell transdifferentiation.

Discussion

The gastric corpus mucosa contains 6 types of differentiated cells: parietal cells, chief cells, surface mucous cells, mucous neck cells, tuft cells, and enteroendocrine cells. All cells originate from stem cells in the isthmus region, but mucous neck cells can function as an intermediate precursor for chief cells.[16] The differentiation process from mucous neck cells into chief cells involves dynamic alterations, including granule changes from mucous to serous, the alteration of apical-basal cell shape organization, and the expansion of rough endoplasmic reticulum.[16,31] MIST1 and its upstream gene XBP1 are transcription factors that regulate the cellular architecture maturation in chief cells.[16] In addition, parietal cell loss induces the transdifferentiation of chief cells into mucous cell metaplasia, designated SPEM.[32] In this study, we have demonstrated the involvement of miR-148a in the process of transdifferentiation of chief cells into SPEM. In situ hybridization analyses showed that miR-148a was specifically expressed in normal chief cells compared with mucous neck cells. In addition, miR-148a was significantly down-regulated in chief cells during SPEM development. Therefore, miR-148a could be involved in chief cell maturation and maintenance as well as plasticity.

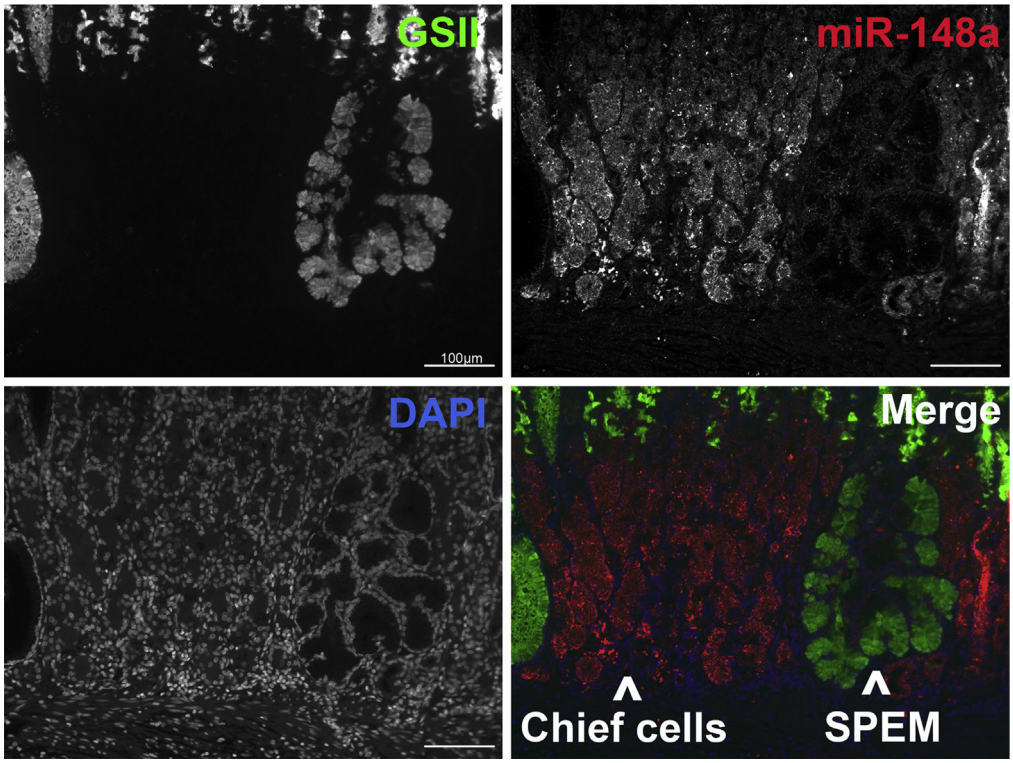

Figure 4. miR-148a expression in human stomach. Fluorescence in situ hybridization for miR-148a (*red*) and immunofluorescence staining for GSII (*green*) and DAPI (*blue*). miR-148a was strongly expressed at the base of the normal glands below the GSII-positive mucous neck cells. The SPEM glands, marked with GSII-positive staining to the base of the glands, had no or little expression of miR-148a.

The extremely high expression of several miRNAs in chief cells suggested that miRNAs could also be involved in chief cell maturation and maintenance in addition to chief cell plasticity. The report that XBP1 can directly induce the transcription of miR-148a supports this hypothesis.[33] However, we did not find that miR-148a can increase chief cell factors in ImChief cells (data not shown). These results suggest that the down-regulation of miR-148a might lead chief cells toward transdifferentiation into SPEM cells. To understand the role of miRNAs on chief cell maturation, other experiments such as the use of mouse models with the deletion of miR-148a specifically in chief cells will be needed.

To investigate chief cell plasticity, we performed experiments using the ImChief cell line that we previously established.[26] The ImChief cell line allows studies to be conducted in an in vitro model that resembles in vivo chief cells. The ImChief cell line also allows for the study of chief cell factors, which are difficult to study with gastric cancer cell lines and mouse models, although ImChief cells are not functionally fully mature.[26] In this study, we also showed that ImChief cells can be transfected effectively with miRNA inhibitors. The list of miRNAs down-regulated during chief cell transdifferentiation included miR-148a and members of the miR-30, miR-200, and let-7 families. Among them, we examined the role of miR-148a in chief cell plasticity. A number of studies have shown that miR-148a is down-regulated in human cancer tissues, including gastric cancer.[28,34–37] These previous investigations have demonstrated that miR-148a down-regulation could contribute to human gastric cancer progression by directly targeting MMP7, DNMT1, CCK-BR, and ROCK1.[38–42] This study suggests a role of miR-148a on the normal physiology of gastric chief cells.

DNA methylation is a major modulator of gene expression. In mammalian cells, methylation is catalyzed by DNMTs that cooperatively establish tissue-specific methylation patterns. DNMT1 is responsible for the maintenance of DNA methylation during replication.[43] Previous reports demonstrated that aberrant DNA methylation is induced in human and Mongolian gerbil gastric mucosa by *H pylori* infection,[44–46] suggesting that regulation of gene expression by DNA methylation could be related with the initiation of metaplasia and neoplasia development. However, the up-regulation of DNMTs has not been observed in human or gerbil gastric mucosa with *H pylori* infection.[45,46] In this report, we demonstrated that Dnmt1 is up-regulated in chief cells during chief cell transdifferentiation via the down-regulation of miR-148a.

Previous studies have demonstrated that miR-148a directly targets the 3′-untranslated region of DNMT1 in various cancer cell lines.[28–30] In contrast, overexpression of DNMT1 leads to hypermethylation of the promoter region of miR-148a in some cancer cell lines, including gastric cancer lines.[28,47] Thus, the regulatory network between miRNAs and epigenetic pathways seems to be important to organize gene expression in cancer biology. In this study, Dnmt1 was up-regulated in chief cells by the suppression of miR-148a especially at early stages of SPEM development. We have previously noted that transdifferentiating chief cells

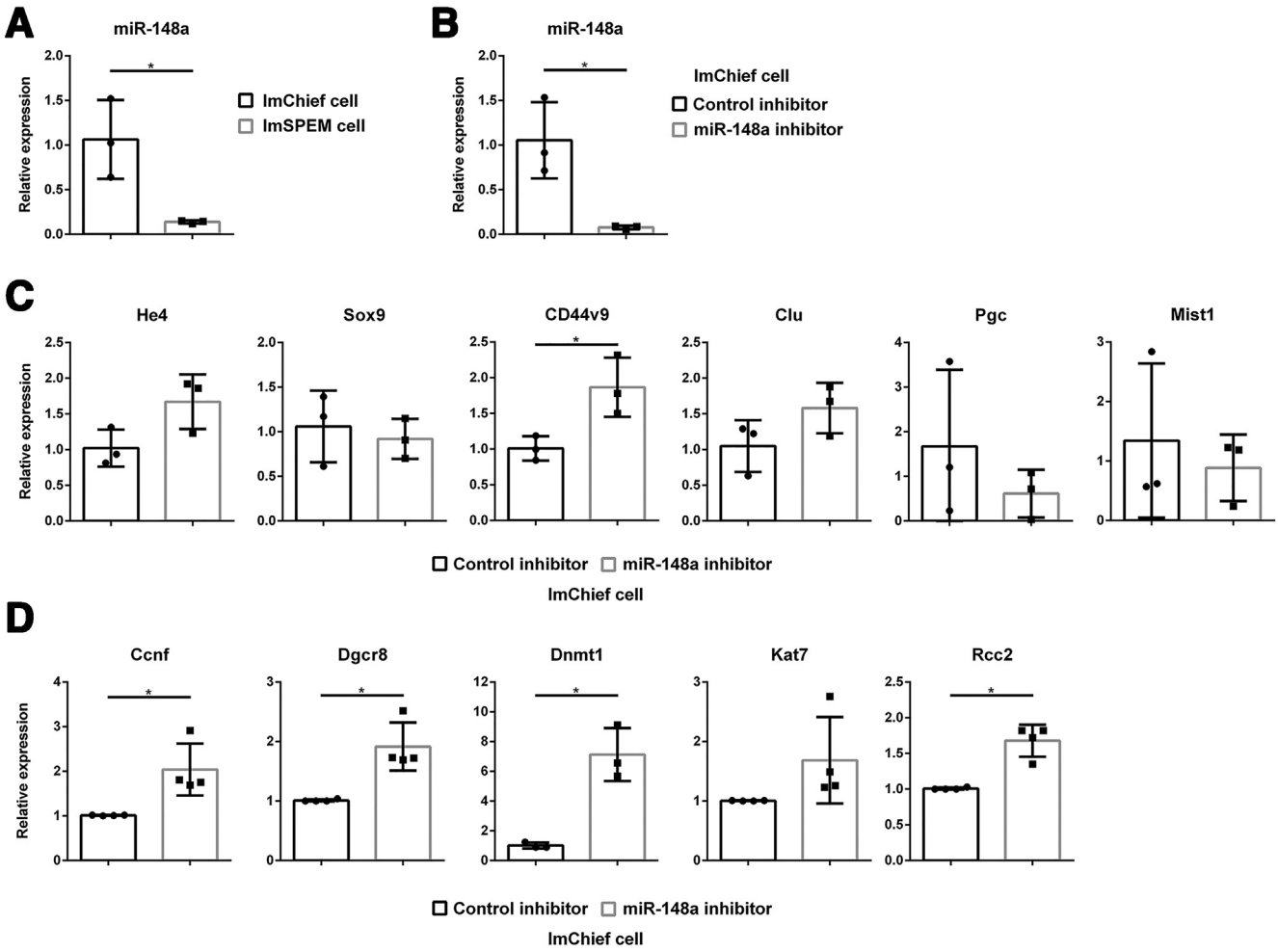

Figure 5. Involvement of miR-148a in initiation of chief cell transdifferentiation. (*A*) Expression of miR-148a in ImChief cells and ImSPEM cells by microRNA assay. Mann-Whitney *U* test, **P* < .05. (*B*) Expression of miR-148a by microRNA assay in ImChief cells treated with control inhibitor or miR-148a inhibitor. Mann-Whitney *U* test, **P* < .05. (*C*) Expression of genes related with SPEM cells (*He4*, *Sox9*, *Cd44v9,* and *Clu*) or chief cells (*Pgc* and *Mist1*) in ImChief cells treated with control inhibitor or miR-148a inhibitor by quantitative PCR. Mann-Whitney *U* test, **P* < .05. (*D*) Expression of miR-148a target genes in ImChief cells treated with control inhibitor or miR-148a inhibitor by quantitative PCR. Mann-Whitney *U* test, **P* < .05.

up-regulate a number of proteins involved in unwinding DNA, which is consistent with a need to reprogram the cell transcriptome.[27] The fact that transdifferentiating chief cells show Dnmt1 up-regulation indicates that the induction of DNA methylation could be necessary for the transdifferentiation of chief cells. To identify methylated genes related with SPEM development, further detailed methylation analyses of chief cells and SPEM cells such as a global methylation analysis are needed at different stages of transdifferentiation.

Interestingly, the down-regulation of miR-148a correlated not only with its target gene, DNMT1, but also with the up-regulation of CD44v9, an early SPEM cell marker, in chief cells. CD44v9 expression is observed in human gastric cancer tissues and has been implicated as a cancer stem cell marker.[48,49] Importantly, SPEM is also associated with the up-regulation of CD44s as well as CD44v9,[18,50] whereas CD44v9 is not expressed in any cells in the normal gastric corpus

Table 4. Candidate MicroRNAs and their Targeted Genes Related to SPEM Development

Candidate miRNAs (miRNA seq data)	Possible targeted genes up-regulated in early stage of SPEM (Nozaki et al[27])
miR-148a	Ccnf Dgcr8 Dnmt1 Kat7 Rcc2
let-7f/7i	Limd2 Rdh10 Thoc1 Myo1f
miR-200b/200c	Rdh10 Dnajc5 Pou6f1 BC037034
miR-192	Ereg Thoc1
miR-200a	Csnk2a1 E2f3 Nme1 Sdf2 Sft2d2 Src
miR-182	Nup155 Rasa1
miR-183	(-)
miR-27b	Plekhh1 Nek6 Litaf Gpd1 Nfx1 Timm8a1
miR-30a/30c	Sdad1 Vat1 Xpo1 Arl6ip5 Mboat1 Poldip3

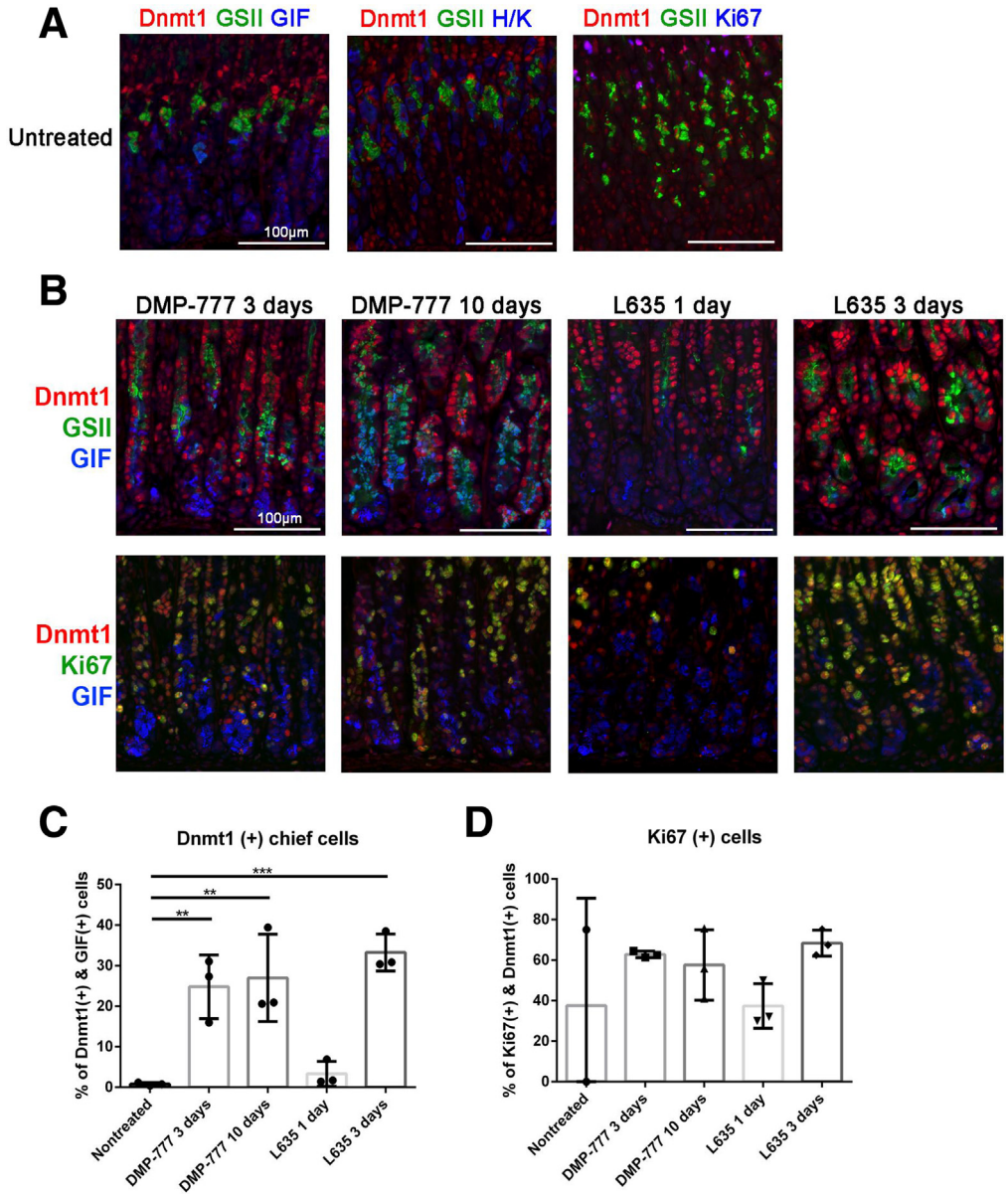

Figure 6. Up-regulation of Dnmt1 in chief cells during chief cell transdifferentiation via down-regulation of miR-148a. (*A*) Immunofluorescence staining in the corpus of untreated mice. *Left panel*: GSII (*green*), Dnmt1 (*red*), and GIF (*blue*). *Middle panel*: GSII (*green*), Dnmt1 (*red*), and H/K-ATPase (*blue*). *Right panel*: GSII (*green*), Dnmt1 (*red*), and Ki67 (*blue*). Dnmt1 was strongly expressed in isthmus cells and neck cells. Dnmt1-positive isthmus cells were positive for Ki67, but Dnmt1-positive mucous neck cells were negative for Ki67. (*B*) Immunofluorescence staining in the corpus of mice treated by DMP-777 for 3 days or 10 days and L635 for 1 day or 3 days. *Upper panel*: GSII (*green*), Dnmt1 (*red*), and GIF (*blue*). Dnmt1 was up-regulated in SPEM cells of mice treated with DMP-777 for 10 days or L635 for 3 days as well as in chief cells of mice treated with DMP-777 for 3 days or L635 for 1 day. *Lower panel*: Ki67 (*green*), Dnmt1 (*red*), and GIF (*blue*). Ki67 was expressed in Dnmt1-positive SPEM cells of mice treated with DMP-777 for 10 days or L635 for 3 days as well as in Dnmt1-positive chief cells of mice treated with DMP-777 for 3 days or L635 for 1 day. (*C*) Quantitation of Dnmt1-positive chief cells. Percent of GIF-positive chief cells per corpus glands that are Dnmt1-positive. One-way analysis of variance, $P = .0003$. Bonferroni multiple comparisons, $^{**}P < .01$, $^{***}P < .001$. (*D*) Quantitation of Ki67 in Dnmt1-positive chief cells. Percent of Dnmt1-positive chief cells per corpus glands that are Ki67-positive.

mucosa. CD44v9 functions by blocking the stress signaling induced by reactive oxygen species via the interaction with the cystine transporter xCT.[19,20] Our recent report identified xCT as required for the SPEM development and chief cell reprogramming after injury and showed that xCT deficiency blocks the transdifferentiation process.[19] Targeting xCT arrested chief cell reprogramming at a specific step where the transdifferentiation was initiated, marked by loss of Mist1, but up-regulation of autophagy did not occur. Investigation of miR-148a expression at this early step in chief cell transdifferentiation confirmed that miR-148a down-regulation occurs early in the initiation of chief cell reprogramming.

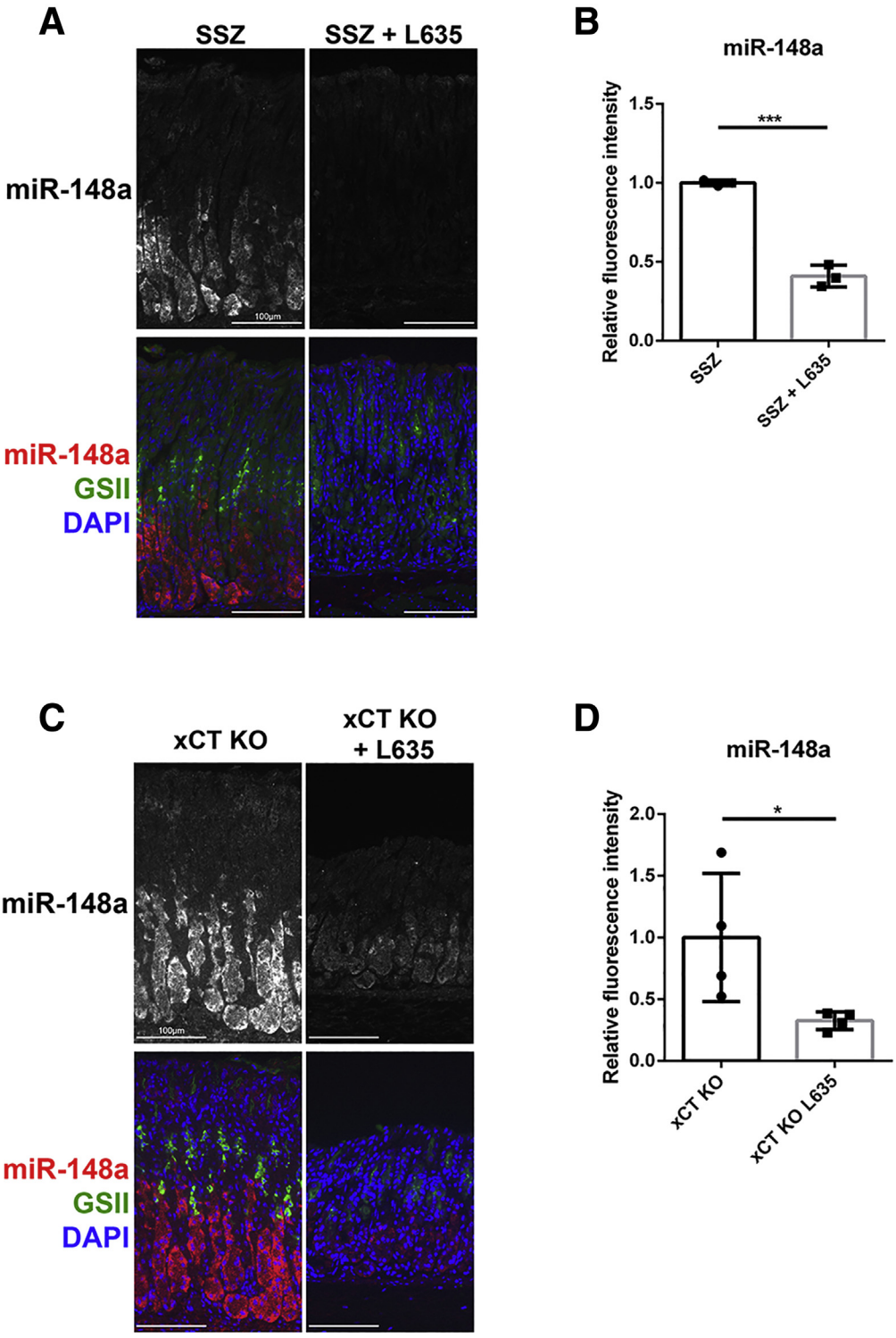

Figure 7. miR-148a down-regulation during chief cell trans-differentiation process. (*A*) Fluorescence in situ hybridization for miR-148a (*red*) and immunofluorescence staining for GSII (*green*) and DAPI (*blue*). miR-148a was expressed in chief cells treated with xCT inhibitor, sulfasalazine, only. With 3 days of L635 co-treatment with sulfasalazine, miR-148a expression was lost. (*B*) Quantitation of relative miR-148a staining intensity. Mann-Whitney *U* test, $^{*}P < .05$. (*C*) Fluorescence in situ hybridization for miR-148a (*red*) and immunofluorescence staining for GSII (*green*) and DAPI (*blue*). In xCT knockout (KO) mice, miR-148a was expressed in chief cells. With 3 days of L635, miR-148a expression was decreased in xCT KO mice. (*D*) Quantitation of relative miR-148a staining intensity. Mann-Whitney *U* test, $^{*}P < .05$.

Metaplasia is considered to be a precursor lesion for gastric cancer; however, the mechanisms of how metaplasia develops in stomach are not fully elucidated. The mouse models of induced acute parietal cell loss such as DMP-777, L635, and high-dose tamoxifen have shown that chief cells can give rise to SPEM cells via a transdifferentiation process.[21,32,51] Recent analyses suggest that parietal cell loss alone is not sufficient to induce metaplasia,[52] and another signaling process, such as the interleukin 33/interleukin 13 cytokine signaling network, is required for SPEM development.[17] The results from this study indicate that post-transcriptional regulation by miR-148a could be

Table 5. Primer Sequences for Quantitative PCR

Primer name	Sequence
Tbp F	CAAACCCAGAATTGTTCTCCTT
Tbp R	ATGTGGTCTTCCTGAATCCCT
He4 F	TGCCTGCCTGTCGCCTCTG
He4 R	TGTCCGCACAGTCCTTGTCCA
Sox9 F	CACGGAGCAGACGCACATCT
Sox9 R	TCTCGCTTCAGGTCAGCCTT
Cd44v9 F	GGAGATCAGGATGACTCCTTCT
Cd44v9 R	AGTCCTTGGATGAGTCTCGATC
Clu F	CCAGCCTTTCTTTGAGATGA
Clu R	CTCCTGGCACTTTTCACACT
Pgc F	TCTAACGGCGGGCAGATT
Pgc R	AGGTACTGGGCAGGCATGAC
Mist1 F	GCTGACCGCCACCATACTTAC
Mist1 R	TGTGTAGAGTAGCGTTGCAGG
Dnmt1 F	AGATGCCATCACCCAAAAAG
Dnmt1 R	TCATCGATGCTCACCTTCTG
Tff2 F	TGCTTTGATCTTGGATGCTG
Tff2 R	GGAAAAGCAGCAGTTTCGAC
Ccnf F	CACACCAGCCTGTCCATCTATG
Ccnf R	ACGAGGTCACTGTAGGAGAAGC
Dgcr8 F	GATGGTGTGACTTACGGATCTGG
Dgcr8 R	TAGGCTTCTCCTCAGAGGTCTG
Kat7 F	AGGAAAAGGTGGCTGAACTCAGG
Kat7 R	GTCAGGTTTTCCAAGAGAGGCTC
Rcc2 F	GTGGTTCGAGATGTAGCCTGTG
Rcc2 R	AGGCACCATCTCATCCTTCTGC

involved in the chief cell transdifferentiation by regulating DNMT1 expression and epigenetic change. Moreover, the miR-148a down-regulation triggered in response to mucosal injury occurred very early in the chief cell transdifferentiation process. The miR-148a inhibition in vitro using ImChief cell lines also supported this notion, because miR-148a inhibition alone was sufficient to induce up-regulation of CD44v9 transcripts in chief cells. The rapid down-regulation of miR-148a, especially from such a high level of expression in normal chief cells, would be expected to result in a cascade of targeted events, and the early change in miR-148a expression suggests that miR-148a down-regulation could play a crucial role in the initiation of chief cell reprogramming.

Materials and Methods

Mice

Eight-week-old C57BL/6 mice were used for all mouse experiments. For drug treatment experiments, 3 mice were used per group. DMP-777 and L635 treatment and dosage were conducted as previously described.[15,32] Briefly, DMP-777 was dissolved in 1% methylcellulose and administered by oral gavage (350 mg/kg) once a day for 3 or 10 consecutive days. L635 was dissolved in deionized DNA and RNA-free water and administered by oral gavage (350 mg/kg) once a day for 1 or 3 consecutive days. Mist1$^{CreERT2/+}$ mice were crossed with R26R^{mTmG} or R26R^{tdTomato} mice, and 5 mg tamoxifen was administered to these mice subcutaneously every other day for 3 total doses.

Archival sections of stomach from *H felis* infected, sulfasalazine treated, and xCT knockout mice were obtained from previous study.[15,19] Regular mouse chow and water ad libitum were provided during experiments in a temperature-controlled room with 12-hour light-dark cycles. All treatment maintenance and care of animals in these studies followed protocols approved by the Institutional Animal Care and Use Committees of Vanderbilt University.

Cell Lines

Mouse chief cell line (ImChief cell) and SPEM cell line (ImSPEM cell) were established in a previous study.[26] These cell lines were maintained in a 1:1 mixture of Ham's F-12 and Dulbecco minimum essential medium (DMEM) containing 10% fetal bovine serum, 8 μg/mL insulin/transferrin/selenium solution, 1 μg/mL hydrocortisone, 100 U/mL penicillin and streptomycin, 100 μg/mL MycoZap Plus-PR, 1 ng/mL epidermal growth factor, 1 ng/mL basic fibroblast growth factor, and 5 U/mL interferon-γ. For ongoing maintenance, these cells were incubated and passaged at the permissive temperature (33°C). For analyses of experiments, cells were incubated at the non-permissive temperature (39°C) for 72 hours.

Total RNA Reparation From In Vivo Chief Cells and Chief Cell or Spasmolytic Polypeptide-Expressing Metaplasia Cell Lines for MicroRNA Sequencing

Mist1$^{CreERT2/+}$ mice were crossed with R26R^{mTmG} reporter mice, and 2 Mist1$^{CreERT2/+}$;R26R$^{mTmG/+}$ mice were used for chief cell isolation. Mice were killed 10 days after tamoxifen injection. The stomachs were removed and opened along the greater curvature. Stomachs were rinsed with ice-cold phosphate-buffered saline without Ca and Mg, and the antrums were removed with a razor blade and discarded. The corpus mucosa was separated from the serosa by dragging a cell scraper along the muscle layer. The corpus mucosa was minced with scissors and digested in the buffer containing advanced DMEM/F12, 5% fetal bovine serum, 1 mg/mL collagenase type Ia, and DNase I at 37°C. Advanced DMEM/F12 supplemented with 10 μmol/L Y-27632 and 1 mmol/L dithiothreitol was added to stop the reaction. These cells were resuspended in cold TrypLE Express supplemented with Y-27632 and incubated at 37°C. After stopping reaction, cells were resuspended in advanced DMEM/F12 with 1% fetal bovine serum and DNase I supplemented with Y-27632. Before cell sorting, cells were incubated with 1.0 μg/mL 4′,6-diamidino-2-phenylindol (DAPI). Cells were sorted by using a BD fluorescence-activated cell sorting Aria III (BD Biosciences, San Jose, CA) and initially segregated from debris by using forward scatter and side scatter properties of the 488-nm laser. Single cells were selected using the voltage pulse geometries

of the forward scatter diode and side scatter photomultiplier tube detectors. Dead cells were excluded on the basis of their DAPI staining. GFP-positive chief cells were sorted directly into TRIzol (Invitrogen, Carlsbad, CA) using a 100-μm nozzle, followed by total RNA extraction according to the manufacturer's instructions.

Total RNA extraction from chief cell lines and SPEM cell lines for miRNA sequencing and ImChief cells and ImSPEM cells grown at the non-permissive temperature were collected from 80% confluent T-75 dish. Cells were trypsinized, washed with phosphate-buffered saline twice, and pelleted. Total RNA was extracted by using the miRVana miRNA Isolation Kit according to manufacturer's instructions.[14]

MicroRNA Library Preparation, Sequencing, and Data Analysis

Total RNA from each sample was processed through an RNA library preparation protocol using NEBNext Small RNA Library Prep Set for Illumina (New England BioLabs Inc, Ipswich, MA) according to manufacturer's protocol. Briefly, 3′ adapters were ligated to total input RNA, followed by hybridization of multiplex SR RT primers and ligation of multiplex 5′ SR adapters. Reverse transcription was done using ProtoScript II RT for 1 hour at 50°C. Immediately after reverse transcription reaction, PCR amplification was performed for 15 cycles using LongAmp Taq 2X master mix. Illumina indexed primers were added to uniquely barcode each sample. Post-PCR material was purified by using QIAquick PCR purification kit (Qiagen Inc, Valencia, CA). Size selection of small RNA was done using 3% agarose free gel cassettes on Pippin prep instrument (Sage Science Inc, Beverly, MA). Post-size selection concentration and quality of the libraries were assessed by using Qubit 2.0 Fluorometer (Invitrogen) and DNA 1000 chip on Agilent 2100 Bioanalyzer (Applied Biosystems, Carlsbad, CA), respectively. Accurate quantification for sequencing applications was performed by using the quantitative PCR-based KAPA Biosystems Library Quantification kit (Kapa Biosystems, Inc, Woburn, MA). Each library was diluted to a final concentration of 1.25 nmol/L and pooled in equimolar ratios before clustering. Single End sequencing (50 base pairs) was performed to generate approximately 15 million reads per sample on an Illumina HiSeq2500 sequencer (Illumina, Inc, San Diego, CA).

Post-processing of the sequencing reads from miRNA-seq experiments from each sample was performed as per the Genomic Services Laboratory unique in-house pipeline. Briefly, quality control checks on raw sequence data from each sample were performed by using FastQC (Babraham Bioinformatics, London, UK). Raw reads were imported on a commercial data analysis platform AvadisNGS (Strand Scientifics, CA). Adapter trimming was done to remove ligated adapter from 3′ end of the sequenced reads, with only one mismatch allowed; poorly aligned 3′ ends were also trimmed. Sequences shorter than 15 nucleotides length were excluded from further analysis. Trimmed reads with low qualities (base quality score less than 30, alignment score less than 95, mapping quality less than 40) were removed. Filtered reads were then used to extract and count the small RNA, which was annotated with miRNAs from the miRBase release 20 database. The quantification operation carries out measurement at the gene level and at the active region level. Active region quantification considers only reads whose 5′ end matches the 5′ end of the mature miRNA annotation. For comparison of ImChief and ImSPEM cells, samples were grouped as identifiers, and the differential expression of miRNA was calculated on the basis of their fold change observed between different groups; *P* value of differentially expressed miRNAs was estimated by implementing z-score calculations using Benjamini Hochberg FDR corrections of 0.05.[53]

Immunofluorescence Staining

Mouse stomachs were fixed in 4% paraformaldehyde overnight and transferred into 70% ethanol for paraffin embedding. Five-micrometer paraffin-embedded sections were used for all immunofluorescence staining. Sections were deparaffinized, rehydrated, and submitted to antigen retrieval using Target Retrieval solution (Dako North America, Inc, Carpinteria, CA) in a pressure cooker. Blocking was performed by using Protein Block Serum-Free (Dako North America, Inc) for 1 hour 30 minutes at room temperature. The primary antibody incubation was performed in Antibody Diluent with Background Reducing Components (Dako North America, Inc) overnight at 4°C. Primary antibodies used were as follows: rat anti-Cd44v9 (1:25,000), goat anti-GIF (1:2000), rabbit anti-Mist1 (1:300), mouse anti-HK-ATPase (1:10,000), rat anti-Ki67 (1:50), and rabbit anti-Dnmt1 (1:200). Fluorescent second antibodies (1:500) and Alexa-488 and 647-conjugated GSII (1:2000) were incubated for 1 hour at room temperature. After incubation with DAPI for 5 minutes, slides were mounted with ProLong Gold Antifade Reagent (Invitrogen). Fluorescence imaging was analyzed by using an Axio Imager 2 microscope (Carl Zeiss AG, Oberkochen, Germany) or a Versa S200 automated slide scanner (Leica Biosystems, Buffalo Grove, IL) in the Vanderbilt Digital Histology Shared Resource.

Fluorescence In Situ Hybridization for MiR-148a

Stomachs of wild-type mice were fixed in 4% paraformaldehyde overnight and transferred into 70% ethanol for paraffin embedding. Five-micrometer paraffin-embedded sections were deparaffinized and rehydrated. Stomachs of $Mist1^{CreERT2/+}$;$R26R^{tdTomato/+}$ mice were fixed in 4% paraformaldehyde overnight and embedded in OCT compound. Ten-micrometer sections were cut from OCT-embedded blocks, mounted on SuperFrost Plus slides, allowed to air-dry for 15 minutes, and then rinsed for 3 × 3 minutes. In situ hybridization process and TSA Plus fluorescence system were performed as the manufacturer's protocol from Exiqon (South Korea). Briefly, incubation with proteinase-K (2 μg/mL) was performed for 10 minutes at 37°C. Then blocking of endogenous peroxidase activity was performed by using peroxidase block (Dako) for 10 minutes at room temperature. In situ hybridization was performed

by using locked nucleic acid probes (25 nmol/L) for 1 hour at 60°C. After washing slides in side scatter buffers, blocking was conducted by using 1% sheep serum for 15 minutes at room temperature. Anti-digoxigenin-POD antibody (1:400) was applied to slides and incubated for 1 hour at room temperature. To detect digoxigenin, TSA Plus Cy5 substrate (1:200) was applied to slides and incubated for 10 minutes at room temperature. After incubation with Alexa-488 conjugated GSII (1:2000) for 30 minutes and DAPI for 5 minutes, slides were mounted with ProLong Gold Antifade Reagent (Invitrogen).

To examine the localization of miRNAs and proteins, a combination analysis with in situ hybridization for miRNAs and immunofluorescence staining for proteins was performed. Five-micrometer paraffin-embedded sections were deparaffinized, rehydrated, and submitted to antigen retrieval using Target Retrieval solution (Dako North America, Inc) in a pressure cooker. Blocking of endogenous peroxidase activity, in situ hybridization, protein blocking with sheep serum, incubation with anti-digoxigenin-POD, and incubation with TSA plus Cy5 were performed as noted above. Then slides were blocked by using Protein Block Serum-Free (Dako North America, Inc) and incubated with primary and secondary antibodies as in the regular immunofluorescence staining method.

MicroRNA Transfection Experiments

ImChief cells were transfected with 100 nmol/L miRNA inhibitors (miR-148a or control inhibitor) by using Lipofectamine 2000 reagent (Invitrogen) at 33°C, incubated at 33°C for 24 hours, and then cultured at 39°C for 72 hours. Total RNA was extracted from ImChief cells or ImSPEM cells with TRIzol (Invitrogen) according to the manufacturer's instructions. For quantitative reverse transcription PCR of mRNA, 1 μg total RNA was treated with RQ1 RNase-free DNase (Promega, Madison, WI) and then reverse-transcribed with Superscript III reverse transcriptase (Invitrogen). Quantitative real-time PCR was performed with SYBR Green by using specific primers (Table 5) in triplicate using an ABI StepOnePlus Real-Time PCR System (Applied Biosystems). A set of PCR primers for TATA-box-binding protein (Tbp) gene was used as an endogenous control and reference for verification of sufficient cDNA in the reaction. Each sample was collected from at least 3 biological replicate experiments. The miRNA expression in cell lysates was analyzed by using TaqMan MicroRNA assays according to the manufacturer's instructions. U6 was used as an endogenous control. Statistical significance ($P < .05$) of the differences in the expression levels was determined with Mann-Whitney U test.

Image Quantitation

For miR-148a expression, experimental groups contained 3–8 mice. Images were analyzed with CellProfiler by using total intensity divided by the area detected, and all graphs and statistics were completed in GraphPad Prism (San Diego, CA). The intensity and area were calculated by masking out all areas except the base of the gland. More than 100 glands of proximal stomach corpus were taken from each mouse at ×20 objective for quantification. For acute and chronic mouse model of SPEM, one-way analysis of variance and Bonferroni multiple comparisons test were used to calculate statistical significance ($P < .05$). For xCT deficiency mouse model, the Mann-Whitney U test was used to determine statistical significance ($P < .05$).

To perform the quantitation of the percentage of Dnmt1-positive cells or Ki67 and Dnmt1 double-positive cells in chief cells or SPEM cells, 30 corpus glands were analyzed for each sample. Three samples were analyzed per group (untreated, DMP-777 treatment for 3 days, DMP-777 treatment for 10 days, L635 treatment for 1 day, and L635 treatment for 3 days). Chief cells were detected as GIF-positive cells. Counting was performed in slides digitally imaged with a Leica Versa 200 scanner (Vanderbilt Digital Histology Shared Resource) or in overlaid fluorescence images using Adobe Photoshop (San Jose, CA). One-way analysis of variance and Bonferroni multiple comparisons test were used to calculate statistical significance ($P < .05$).

References

1. Weis VG, Petersen CP, Weis JA, Meyer AR, Choi E, Mills JC, Goldenring JR. Maturity and age influence chief cell ability to transdifferentiate into metaplasia. Am J Physiol Gastrointest Liver Physiol 2016;312:G67–G76.
2. Goldenring JR, Nam KT, Mills JC. The origin of pre-neoplastic metaplasia in the stomach: chief cells emerge from the Mist. Exp Cell Res 2011; 317:2759–2764.
3. Lennerz JKM, Kim S, Oates EL, Huh WJ, Dherty JM, Tian X, Bredemeyer AJ, Goldenring JR, Lauwers GY, Shin GY, Mills JC. The transcription factor MIST1 is a novel human gastric chief cell marker whose expression is lost in metaplasia, dysplasia and carcinoma. Am J Pathol 2010;177:1514–1533.
4. Bredemeyer AJ, Geahlen JH, Weis VG, Huh WJ, Zinselmeyer BH, Srivatsan S, Miller MJ, Shaw AS, Mills JC. The gastric epithelial progenitor cell niche and differentiation of the zymogenic (chief) cell lineage. Dev Biol 2009;325:211–224.
5. Mills JC, Sansom OJ. Reserve stem cells: differentiated cells reprogram to fuel repair, metaplasia, and neoplasia in the adult gastrointestinal tract. Sci Signal 2015;8:re8.
6. Goldenring JR, Nam KT, Wang TC, Mills JC, Wright NA. Spasmolytic polypeptide-expressing metaplasia and intestinal metaplasia: time for reevaluation of metaplasias and the origins of gastric cancer. Gastroenterology 2010; 138:2207–2210.
7. Bartel DP. MicroRNAs: genomics, biogenesis, mechanism, and function. Cell 2004;116:281–297.
8. Ha M, Kim VN. Regulation of microRNA biogenesis. Nat Rev Mol Cell Biol 2014;15:509–524.
9. Esquela-Kerscher A, Slack FJ. Oncomirs: microRNAs with a role in cancer. Nat Rev Cancer 2006;6:259–269.
10. Calin GA, Croce CM. MicroRNA signatures in human cancers. Nat Rev Cancer 2006;6:857–866.
11. Ueda T, Volinia S, Okumura H, Shimizu M, Taccioli C, Rossi S, Alder H, Liu CG, Oue N, Yasui W, Yoshida K,

Sasaki H, Nomura S, Seto Y, Kaminishi M, Calin GA, Croce CM. Relation between microRNA expression and progression and prognosis of gastric cancer: a microRNA expression analysis. Lancet Oncol 2010; 11:136–146.
12. Matsushima K, Isomoto H, Inoue N, Nakayama T, Hayashi T, Nakayama M, Nakao K, Hirayama T, Kohno S. MicroRNA signatures in Helicobacter pylori-infected gastric mucosa. Int J Cancer 2011;128:361–370.
13. Zabaleta J. MicroRNA: a bridge from H pylori infection to gastritis and gastric cancer development. Frontiers in Genetics 2012;3:294.
14. Sousa JF, Nam KT, Petersen CP, Lee HJ, Yang HK, Kim WH, Goldenring JR. miR-30-HNF4gamma and miR-194-NR2F2 regulatory networks contribute to the upregulation of metaplasia markers in the stomach. Gut 2016; 65:914–924.
15. Weis VG, Sousa JF, LaFleur BJ, Nam KT, Weis JA, Finke PE, Ameen NA, Fox JG, Goldenring JR. Heterogeneity in mouse SPEM lineages identifies markers of metaplastic progression. Gut 2013;62:1270–1279.
16. Ramsey VG, Doherty JM, Chen CC, Stappenbeck TS, Konieczny SF, Mills JC. The maturation of mucus-secreting gastric epithelial progenitors into digestive-enzyme secreting zymogenic cells requires Mist1. Development 2007;134:211–222.
17. Petersen CP, Meyer AR, De Salvo C, Choi E, Schlegel C, Petersen A, Engevik AC, Prasad N, Levy SE, Peebles RS, Pizarro TT, Goldenring JR. A signalling cascade of IL-33 to IL-13 regulates metaplasia in the mouse stomach. Gut 2018;67:805–817.
18. Wada T, Ishimoto T, Seishima R, Tsuchihashi K, Yoshikawa M, Oshima H, Oshima M, Masuko T, Wright NA, Furuhashi S, Hirashima K, Baba H, Kitagawa Y, Saya H, Nagano O. Functional role of CD44v-xCT system in the development of spasmolytic polypeptide-expressing metaplasia. Cancer Science 2013;104:1323–1329.
19. Meyer AR, Engevik AC, Willet SG, Williams JA, Zou Y, Massion PP, Mills JC, Choi E, Goldenring JR. Cystine/glutamate antiporter (xCT) is required for chief cell plasticity after gastric injury. Cell Mol Gastroenterol Hepatol 2019;8:379–405.
20. Ishimoto T, Nagano O, Yae T, Tamada M, Motohara T, Oshima H, Oshima M, Ikeda T, Asaba R, Yagi H, Masuko T, Shimizu T, Ishikawa T, Kai K, Takahashi E, Imamura Y, Baba Y, Ohmura M, Suematsu M, Baba H, Saya H. CD44 variant regulates redox status in cancer cells by stabilizing the xCT subunit of system xc(-) and thereby promotes tumor growth. Cancer Cell 2011;19:387–400.
21. Willet SG, Lewis MA, Miao ZF, Liu D, Radyk MD, Cunningham RL, Burclaff J, Sibbel G, Lo HG, Blanc V, Davidson NO, Wang ZN, Mills JC. Regenerative proliferation of differentiated cells by mTORC1-dependent paligenosis. EMBO J 2018;37(7).
22. Qiu X, Zhu H, Liu S, Tao G, Jin J, Chu H, Wang M, Tong N, Gong W, Zhao Q, Qiang F, Zhang Z. Expression and prognostic value of microRNA-26a and microRNA-148a in gastric cancer. J Gastroenterol Hepatol 2017; 32:819–827.
23. Tsukamoto Y, Nakada C, Noguchi T, Tanigawa M, Nguyen LT, Uchida T, Hijiya N, Matsuura K, Fujioka T, Seto M, Moriyama M. MicroRNA-375 is downregulated in gastric carcinomas and regulates cell survival by targeting PDK1 and 14-3-3zeta. Cancer Res 2010; 70:2339–2349.
24. Tang H, Deng M, Tang Y, Xie X, Guo J, Kong Y, Ye F, Su Q, Xie X. miR-200b and miR-200c as prognostic factors and mediators of gastric cancer cell progression. Clin Cancer Res 2013;19:5602–5612.
25. Motoyama K, Inoue H, Nakamura Y, Uetake H, Sugihara K, Mori M. Clinical significance of high mobility group A2 in human gastric cancer and its relationship to let-7 microRNA family. Clin Cancer Res 2008; 14:2334–2340.
26. Weis VG, Petersen CP, Mills JC, Tuma PL, Whitehead RH, Goldenring JR. Establishment of novel in vitro mouse chief cell and SPEM cultures identifies MAL2 as a marker of metaplasia in the stomach. Am J Physiol Gastrointest Liver Physiol 2014;307:G777–G792.
27. Nozaki K, Ogawa M, Williams JA, LaFleur BJ, Ng V, Drapkin RI, Mills JC, Konieczny SF, Nomura S, Goldenring JR. A molecular signature of gastric metaplasia arising in response to acute parietal cell loss. Gastroenterology 2008;134:511–521.
28. Zhu A, Xia J, Zuo J, Jin S, Zhou H, Yao L, Huang H, Han Z. MicroRNA-148a is silenced by hypermethylation and interacts with DNA methyltransferase 1 in gastric cancer. Med Oncol 2012;29:2701–2709.
29. Gailhouste L, Gomez-Santos L, Hagiwara K, Hatada I, Kitagawa N, Kawaharada K, Thirion M, Kosaka N, Takahashi RU, Shibata T, Miyajima A, Ochiya T. miR-148a plays a pivotal role in the liver by promoting the hepatospecific phenotype and suppressing the invasiveness of transformed cells. Hepatology 2013; 58:1153–1165.
30. Wu T, Qu L, He G, Tian L, Li L, Zhou H, Jin Q, Ren J, Wang Y, Wang J, Kan X, Liu M, Shen J, Guo M, Sun Y. Regulation of laryngeal squamous cell cancer progression by the lncRNA H19/miR-148a-3p/DNMT1 axis. Oncotarget 2016;7:11553–11566.
31. Karam SM, Leblond CP. Dynamics of epithelial cells in the corpus of the mouse stomach: III—inward migration of neck cells followed by progressive transformation into zymogenic cells. Anat Rec 1993;236:297–313.
32. Nam KT, Lee H-J, Sousa JF, Weis VG, O'Neal RL, Finke PE, Romero-Gallo J, Shi G, Mills JC, Peek RM, Konieczny SF, Goldenring JR. Mature chief cells are cryptic progenitors for metaplasia in the stomach. Gastroenterology 2010;139:2028–2037.
33. Cho YM, Kim TM, Hun Kim D, Hee Kim D, Jeong SW, Kwon OJ. miR-148a is a downstream effector of X-box-binding protein 1 that silences Wnt10b during adipogenesis of 3T3-L1 cells. Exp Mol Med 2016;48:e226.
34. Jiang Q, He M, Ma MT, Wu HZ, Yu ZJ, Guan S, Jiang LY, Wang Y, Zheng DD, Jin F, Wei MJ. MicroRNA-148a inhibits breast cancer migration and invasion by directly targeting WNT-1. Oncol Rep 2016;35:1425–1432.
35. Cao H, Liu Z, Wang R, Zhang X, Yi W, Nie G, Yu Y, Wang G, Zhu M. miR-148a suppresses human renal cell

carcinoma malignancy by targeting AKT2. Oncol Rep 2017;37:147–154.
36. Liu L, Ye JX, Qin YZ, Chen QH, Ge LY. Evaluation of miR-29c, miR-124, miR-135a and miR-148a in predicting lymph node metastasis and tumor stage of gastric cancer. International Journal of Clinical and Experimental Medicine 2015;8:22227–22236.
37. Peng L, Liu Z, Xiao J, Tu Y, Wan Z, Xiong H, Li Y, Xiao W. MicroRNA-148a suppresses epithelial-mesenchymal transition and invasion of pancreatic cancer cells by targeting Wnt10b and inhibiting the Wnt/beta-catenin signaling pathway. Oncol Rep 2017;38:301–308.
38. Sakamoto N, Naito Y, Oue N, Sentani K, Uraoka N, Zarni Oo H, Yanagihara K, Aoyagi K, Sasaki H, Yasui W. MicroRNA-148a is downregulated in gastric cancer, targets MMP7, and indicates tumor invasiveness and poor prognosis. Cancer Science 2014;105:236–243.
39. Yan J, Guo X, Xia J, Shan T, Gu C, Liang Z, Zhao W, Jin S. MiR-148a regulates MEG3 in gastric cancer by targeting DNA methyltransferase 1. Med Oncol 2014; 31:879.
40. Yu B, Lv X, Su L, Li J, Yu Y, Gu Q, Yan M, Zhu Z, Liu B. MiR-148a functions as a tumor suppressor by targeting CCK-BR via inactivating STAT3 and Akt in human gastric cancer. PLoS One 2016;11:e0158961.
41. Zheng B, Liang L, Wang C, Huang S, Cao X, Zha R, Liu L, Jia D, Tian Q, Wu J, Ye Y, Wang Q, Long Z, Zhou Y, Du C, He X, Shi Y. MicroRNA-148a suppresses tumor cell invasion and metastasis by downregulating ROCK1 in gastric cancer. Clin Cancer Res 2011;17:7574–7583.
42. Li B, Wang W, Li Z, Chen Z, Zhi X, Xu J, Li Q, Wang L, Huang X, Wang L, Wei S, Sun G, Zhang X, He Z, Zhang L, Zhang D, Xu H, El-Rifai W, Xu Z. MicroRNA-148a-3p enhances cisplatin cytotoxicity in gastric cancer through mitochondrial fission induction and cyto-protective autophagy suppression. Cancer Lett 2017;410:212–227.
43. Perdigoto CN, Valdes VJ, Bardot ES, Ezhkova E. Epigenetic regulation of epidermal differentiation. Cold Spring Harb Perspect Med 2014;4(2).
44. Maekita T, Nakazawa K, Mihara M, Nakajima T, Yanaoka K, Iguchi M, Arii K, Kaneda A, Tsukamoto T, Tatematsu M, Tamura G, Saito D, Sugimura T, Ichinose M, Ushijima T. High levels of aberrant DNA methylation in Helicobacter pylori-infected gastric mucosae and its possible association with gastric cancer risk. Clin Cancer Res 2006;12(Pt 1):989–995.
45. Niwa T, Tsukamoto T, Toyoda T, Mori A, Tanaka H, Maekita T, Ichinose M, Tatematsu M, Ushijima T. Inflammatory processes triggered by Helicobacter pylori infection cause aberrant DNA methylation in gastric epithelial cells. Cancer Res 2010;70:1430–1440.
46. Nakajima T, Yamashita S, Maekita T, Niwa T, Nakazawa K, Ushijima T. The presence of a methylation fingerprint of Helicobacter pylori infection in human gastric mucosae. Int J Cancer 2009;124:905–910.
47. Long XR, He Y, Huang C, Li J. MicroRNA-148a is silenced by hypermethylation and interacts with DNA methyltransferase 1 in hepatocellular carcinogenesis. Int J Oncol 2014;44:1915–1922.
48. Go SI, Ko GH, Lee WS, Kim RB, Lee JH, Jeong SH, Lee YJ, Hong SC, Ha WS. CD44 variant 9 serves as a poor prognostic marker in early gastric cancer, but not in advanced gastric cancer. Cancer Res Treat 2016;48:142–152.
49. Lau WM, Teng E, Chong HS, Lopez KA, Tay AY, Salto-Tellez M, Shabbir A, So JB, Chan SL. CD44v8-10 is a cancer-specific marker for gastric cancer stem cells. Cancer Res 2014;74:2630–2641.
50. Bertaux-Skeirik N, Wunderlich M, Teal E, Chakrabarti J, Biesiada J, Mahe M, Sundaram N, Gabre J, Hawkins J, Jian G, Engevik AC, Yang L, Wang J, Goldenring JR, Qualls JE, Medvedovic M, Helmrath MA, Diwan T, Mulloy JC, Zavros Y. CD44 variant isoform 9 emerges in response to injury and contributes to the regeneration of the gastric epithelium. J Pathol 2017;242:463–475.
51. Leushacke M, Tan SH, Wong A, Swathi Y, Hajamohideen A, Tan LT, Goh J, Wong E, Denil S, Murakami K, Barker N. Lgr5-expressing chief cells drive epithelial regeneration and cancer in the oxyntic stomach. Nat Cell Biol 2017;19:774–786.
52. Burclaff J, Osaki LH, Liu D, Goldenring JR, Mills JC. Targeted apoptosis of parietal cells is insufficient to induce metaplasia in stomach. Gastroenterology 2017; 152:762–766.
53. Benjamini Y, Hochberg Y. Controlling the false discovery rate: a practical and powerful approach to multiple testing. Journal of the Royal Statistical Society Series B (Methodological) 1995;57:289–300.

Received June 18, 2018. Accepted August 22, 2019.

Correspondence
Address correspondence to: James R. Goldenring, MD, PhD, AGAF, Epithelial Biology Center, Vanderbilt University School of Medicine, MRB IV 10435G, 2213 Garland Avenue, Nashville, Tennessee 37232-2733. e-mail: jim.goldenring@vumc.org; fax: (615) 343-1591.

Author contributions
T.S. and Y.S. performed experiments, analyzed data, wrote the manuscript, and prepared figures. E.C., N.P., and C.P.P. performed experiments, analyzed data, and edited the manuscript. J.R.G. developed experimental design, analyzed data, and edited the manuscript.

Conflicts of interest
The authors disclose no conflicts.

Funding
These studies were supported by grants from Department of Veterans Affairs Merit Review Award IBX000930 and NIH RO1 DK071590 and RO1 DK101332 (to J.R.G) and from DOD W81XWH-17-1-0257, AACR 17-20-41-CHOI, and NIH P30 DK058404 (to E.C). T.S. was the recipient of JSPS Postdoctoral Fellowships for Research Abroad. C.P.P. was supported by NIH NRSA Predoctoral Fellowship (F31 DK104600). This work was supported by core resources of the Vanderbilt Digestive Disease Center (NIH P30 DK058404), Translational Pathology Shared Resource (NCI/NIH Cancer Center Support Grant 2P30 CA068485-14), and imaging supported by the Vanderbilt Digital Histology Shared Resource supported by a VA Shared Instrumentation grant (1IS1BX003097).